DECIPHERING FUNCTIONS OF ABERRANT HEMICHANNELS FORMED BY CONNEXIN 26-I30N AND D50Y MUTATIONS

A Thesis Submitted to
the Graduate School of Engineering and Sciences of
İzmir Institute of Technology
in Partial Fulfillment of the Requirements for the Degree of

MASTER OF SCIENCE

in Molecular Biology and Genetic

by
Hande AYPEK

July 2015
İZMİR

We approve the thesis of **Hande AYPEK**

Examining Committee Members

_____

Assist. Prof. Dr. Gülistan MEŞE ÖZÇİVİCİ
Department of Molecular Biology and Genetics,
İzmir Institute of Technology

_____

Assist. Prof. Dr. Özden YALÇIN ÖZUYSAL
Department of Molecular Biology and Genetics,
Izmir Institute of Technology

_____

Assist. Prof. Dr. Güneş ÖZHAN
Izmir Biomedicine and Genome Center,
Dokuz Eylül University

23 July 2015

_____

Assist. Prof. Dr. Gülistan MEŞE ÖZÇİVİCİ
Supervisor, Molecular Biology and Genetics,
İzmir Institute of Technology

_____

Prof. Dr.Ahmet KOÇ
Head of the Molecular Biology
and Genetics Program

_____

Prof. Dr. Bilge KARAÇALI
Dean of the Graduate School of
Engineering and Sciences

ACKNOWLEDGEMENTS

I would like to express my deepest appreciation and thanks to my supervisor Assist. Prof. Dr. Gülistan MEŞE ÖZÇİVİCİ for her guidance, patience, understanding, encouragement, support and helps during my graduate studies. I am also grateful to Meşe-Özçivici Lab members, Öznur BASKAN, Melis OLÇUM, Deniz UĞUR and Özge KARADAS for their laboratory help, ideas and comments about my work. I also want to thank Yalçın-Özuysal Lab members, Burcu EKİNCİ, Cansu KÜÇÜKKÖSE and Burcu FIRATLIGİL for their support and friendship.

In addition, I would like to thank to Assist. Prof. Dr. Engin ÖZÇİVİCİ and Assist. Prof. Dr. Özden YALÇIN ÖZUYSAL for their mentorships. I would also like to thank to IZTECH Biotechnology and Bioengineering Research and Application Center (BIYOMER) for technical support and The Scientific and Technological Research Council of Turkey (TÜBİTAK) for financial support (Grant number 210T035).

Last but not the least, I place on record, my sincere thanks to my family for their support all over my life and moral during my education.

ABSTRACT

DECIPHERING FUNCTIONS OF ABERRANT HEMICHANNELS FORMED BY Cx26-I30N AND D50Y MUTATIONS

Cells need to communicate with each other for maintenance cellular and tissue homeostasis. Gap junctions are channel-forming structures that are formed by docking of two hemichannels on the plasma membrane of adjacent cells. Connexins are subunits of gap junctions. Connexin 26 (Cx26) is one of the connexin isoform and mutations on the Cx26 gene (*GJB2*) cause non-syndromic and syndromic deafness. Keratitis-ichthyosis-deafness (KID) syndrome is one of the syndromic deafness disorders caused by Cx26 mutations. Among these mutations, Cx26-I30N and D50Y missense mutations were shown to form aberrant hemichannels but their effect on protein biosynthesis and functions have not studied. In this study, we aimed to decipher *in vitro* functions of aberrant hemichannels formed by Cx26-I30N and D50Y mutations.

First of all, the effect of Cx26-I30N and D50Y mutations on localization, mRNA expression and protein synthesis properties were investigated in HeLa, N2A and HaCaT cells. Results suggested that Cx26-I30N and D50Y mutants were not able to form gap junction plaques on the plasma membrane and were localized in the Golgi apparatus. In addition, mutations resulted in a reduction in mRNA expression and protein synthesis. After, functional analysis was performed in Cx26-I30N and D50Y transfected N2A and HaCaT cells. Internal Ca^{2+} content measurement, measurement of released ATP, measurement of cell size and apoptosis assays were performed. Ca^{2+} measurement results showed that both Cx26-I30N and D50Y mutations deregulate Ca^{2+} balance in both N2A and HaCaT cells. Result of ATP release assay indicated that ATP amount in the extracellular environment decreased in N2A cells having Cx26-I30N and D50Y clones. Finally, apoptosis assay showed that number of necrotic cells increased when N2A cells were transfected with Cx26-I30N and D50Y constructs. Therefore, it was shown that aberrant hemichannels formed by Cx26-I30N and D50Y mutations may induce necrotic cell death by disrupting Ca^{2+} balance and ATP amount in cells.

ÖZET

CONNEXIN 26 I30N VE D50Y MUTASYONLARININ SEBEP OLDUĞU NORMAL ÇALIŞMAYAN YARIM KANALLARIN FONKSIYONLARININ BELIRLENMESI

Hücresel ve doku dengeleşiminin devamı için hücreler arası iletişim şarttır. Oluklu bağlantılar kanal oluşturan yapılardır ve komşu hücrelerin, hücre zarındaki yarım kanalların birbirine bağlanması sonucu oluşurlar. Connexinler oluklu bağlnatıların yapı proteinleridir. Connexin 26 (Cx26) bir connexin formudur ve Cx26 geninde (*GJB2*) meydana gelen mutasyonlar sendromik ve sendromik olmayan sağirlığa sebep olur. Keratitis-ichthyosis-deafness (KID) Syndrome Cx26 gene mutasyonlarından dolayı meydana gelen bir sendromic hastalıktır. Bu mutasyonlardan Cx26-I30N ve D50Y yanlış anlam mutasyonları anormal çalışan yarım kanal oluşmasına sebep olmuşlardır. Fakat anormal çalışan kanalların protein biyosentezine ve fonksiyonuna etkileri bilinmemektedir. Bu çalışmada, Cx26-I30N ve D50Y mutasyonları tarafından oluşturulan yarım kanalların *in vitro* ortamda fonksiyonlarının belirlenmesi hedeflenmiştir.

Ilk olarak, Cx26-I30N ve D50Y mutasyonlarının hücre içi lokalizasyon, mRNA ifadelenmesi ve protein sentez miktarlarına etkileri HeLa, N2A ve HaCaT hücrelerinde belirlenmiştir. Sonuçlarda, Cx26-I30N ve D50Y mutantları oluklu bağlantı oluşturamazken, Golgi aygıtında birikmiştir. Ayrıca, mutantların mRNA ifadeleri ve protein sentez miktarları düşmüştür. Daha sonra, Cx26-I30N ve D50Y mutasyonlarının fonksiyonel analizleri N2A ve HaCaT hücrelerinde yapılmıştır. Hücre içi Ca^{2+} ölçümü, salınmış ATP ölçümü, hücre boyutu ölçümü ve apoptosiz tahlili yapılan deneylerdendir. Ca^{2+} ölçümü göstermiştir ki Cx26-I30N and D50Y mutasyonları Ca^{2+} dengesini hem N2A hem de HaCaT hücrelerinde bozmaktadir. Ek olarak, salınmış ATP deneyi göstermiştir ki, hücre çevresindeki salınmış ATP miktarı içinde Cx26-I30N ve D50Y klonları olan N2A hücrelerinde düşmüştür. Son olarak yapılan apoptoziz deneyine göre, Cx26-I30N ve D50Y mutasyonlarını içeren N2A hücreleri nekroz olmuşlardır. Sonuçlar göstermiştir ki, anormal çalışan yarim kanallar Ca^{2+} ve ATP dengelerini bozarak, hücrelerin nekroz olmasına sebep olmuştur.

TABLE OF CONTENT

LIST OF FIGURES

LIST OF TABLES

Table **Page**

CHAPTER 1

INTRODUCTION

1.1. Gap Junctions and Hemichannels

There are four types of cellular junctions in eukaryotic cells and each of them has its unique structure and function. Gap junctions are the channel forming junctions and link cytoplasms of adjacent cells directly and facilitate electrical and metabolic coupling. This way, they provide intercellular communication between eukaryotic cells[1]. Both vertebrates and invertebrates have gap junction channels but their structural proteins are different. Connexins are structural proteins in vertebrates, while innexins are the structural proteins of gap junctions in invertebrates[2].

Gap junctions are formed by docking of two hemichannels in head to head orientation on the plasma membrane of neighboring cells (Figure 1.1)[3,4]. Pore size of gap junctions are approximately 1.5 nm in diameter and allow passage of molecules up to 1.2 kDa such as secondary messengers (cAMP, IP_3), ions (K^+, Ca^{2+}) and small metabolites (glucose)[5,6]. In addition, connexins can also form non-junctional hemichannels that can facilitate passage of molecules between the cell interior and the extracellular environment[7]. Hemichannels are thought to participate in paracrine signaling by regulating Ca^{2+} signaling and ATP release[8]. Gap junctions and hemichannels switch between open and closed conformations that can be regulated by pH, voltage, Ca^{2+} and changes in connexin expression (Figure 1.1)[9].

Gap junctions and hemichannels have roles in many cellular processes such as cell differentiation, growth and apoptosis by transferring signaling molecules between adjacent cells and cellular environment[10]. Moreover, passage of molecules between cells and its environment balance cellular homeostasis and cell synchronization[11]. For instance, connexins regulate Ca^{2+} balance between keratinocyte and cellular environment and provide keratinocyte differentiation[12]. In addition, gap junction based intercellular communication is necessary for differentiation and development of mammary gland[13].

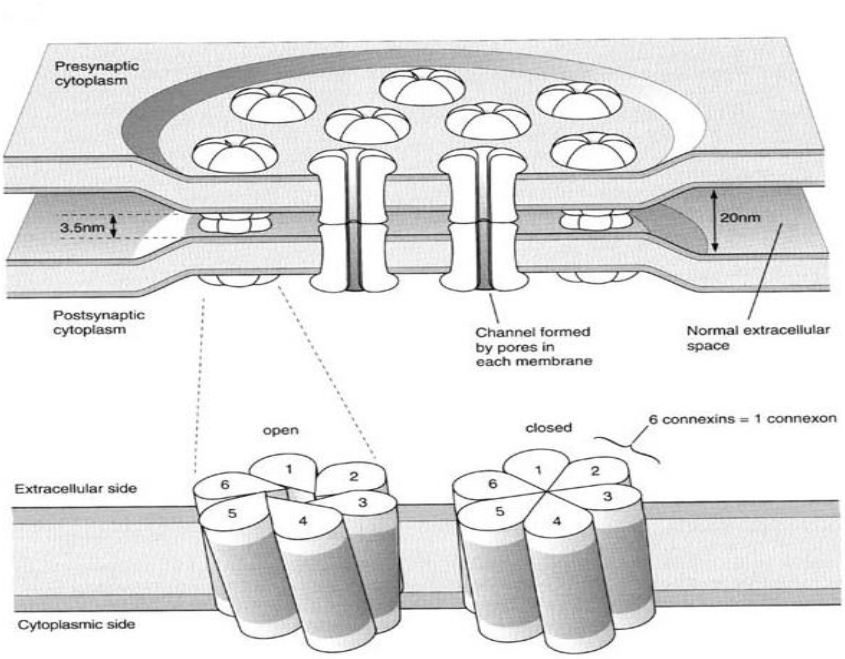

Figure 1.1. Schematic illustration of gap junctions on the plasma membrane. Docking of two hemichannels on the plasma membrane form gap junctions (top). Open and closed forms have different conformations and closure occurs by sliding connexins against each other on clockwise direction (bottom)[4].

1.2. Connexins

Connexins are integral membrane proteins and subunit of gap junctions in vertebrates. Six connexins oligomerize to form hexameric hemichannels known as connexons (Figure 1.2 A)[14]. There are at least 21 connexin isoforms in human[15]. Connexin genes are classified under five gene families based on their phylogenetic origins: alpha, beta, gamma, delta and epsilon[16]. Connexins are named based on their molecular weight such as connexin 26 is 26 kDa or based on their class and discovery order, for example *GJB2 (gap junction beta 2)* also refers to connexin 26 gene which indicates that it is the second discovered connexin in beta family. During the formation of hemichannels, different connexin isoforms can oligomerize to form heteromeric connexons while the same type of connexin isoforms form homomeric connexons (Figure 1.2 C). Similar organization is also observed in the formation of gap junctions where homotypic gap junctions are formed by docking of identical connexon and heterotypic gap junctions include connexons formed from different connexins (Figure 1.2 D)[17,18].

Connexins are highly conserved where each has four transmembrane domains, two extracellular loop, a cytoplasmic loop, an N terminal and a C terminal domains (Figure 1. 2 B)[19]. Transmembrane domains are pore lining regions[20] while, extracellular loops have roles during hemichannel docking[21]. Cytoplasmic loop interacts with the C-terminal domain and regulate hemichannels acidification[22]. The N-terminal domain plays role in voltage gating[23] and the C-terminal domain has role in protein-protein interactions[24].

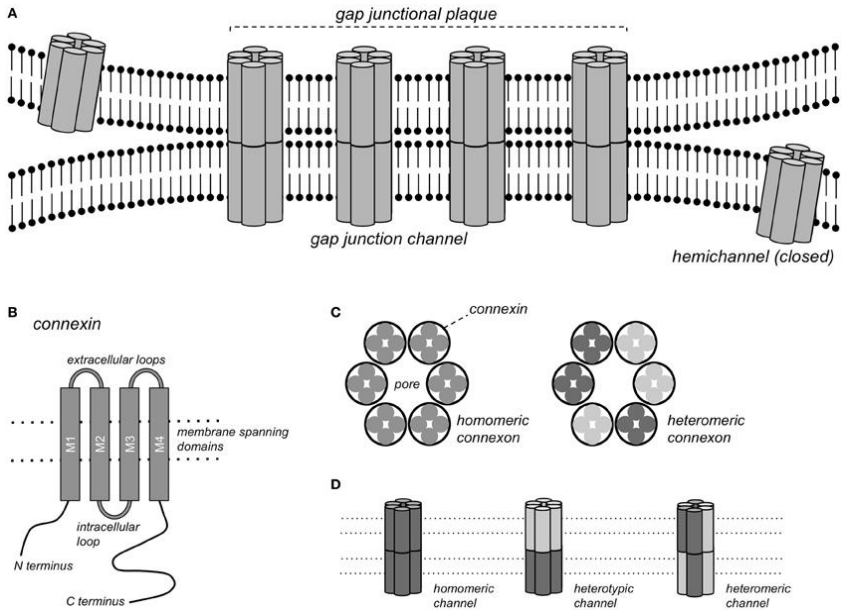

Figure 1.2. Organization of gap junctions. A) Gap junction plaque formation. Gap junction plaques are formed between two adjacent cells to enhance intercellular communication. B) Connexin structure. Connexins have transmembrane domains, two extracellular loop, a cytoplasmic loop, N terminal and C terminal parts. C) Types of hemichannels. Hemichannels are formed in homomeric and heteromeric manner. D) Types of gap junctions. Gap junctions formed in homotypic and heterotypic manner[18].

1.3. Connexin Life Cycle and Connexin Turnover

Connexins are integral membrane proteins and their trafficking to the plasma membrane is facilitated by the secretory pathway (Figure 1.3)[25]. Even though there are some differences in their synthesis and trafficking, the connexin biosynthetic pathways share the similar processes[26]. Connexins are co-translationally synthesized and inserted in the endoplasmic reticulum (ER) membrane. Proper protein folding occurs in ER with

the help of chaperons and misfolded connexins are degraded by proteasomes[27]. Then, correctly folded connexins are transported to the ER-Golgi intermediate compartment (ERGIC) where oligomerization of some connexin isoforms (Cx32) occur to form connexons[28]. For other connexins such as Cx26, Cx43 and Cx46, they are transported from the ERGIC to the Golgi apparatus and their oligomerization to form connexons is completed in the trans-Golgi network (TGN)[29,26]. Finally, connexons are transported to the plasma membrane by secretory vesicles using microtubules[30]. Gap junctions are highly dynamic structures in order to give responses to environmental and physiological stimuli. This quick turnover is mediated by a short half-life of connexins (1.5-5 hours)[9,31]. On the plasma membrane connexons form gap junctions in large number to assemble plaques. Newly synthesized connexins are inserted into the plasma membrane from the peripheral parts of the plaque and internalization of old connexons occurs from the central part of the plaque[32]. During the internalization of gap junctions, only one cell internalizes gap junction or its subunit structures and this double membrane structures are called as "annular junctions" (Figure 1.3)[33]. Annular junctions are internalized by clathrin mediated endocytosis[34] and targeted for different degradation mechanisms. Internalized annular junctions are degraded in lysosomes and proteasome based on their ubiquitin number. Monoubiquitination causes lysosomal and polyubiquitination causes proteasomal degradation[35]. In addition recent studies showed that autophagy is another degradation mechanism for annular junctions[36].

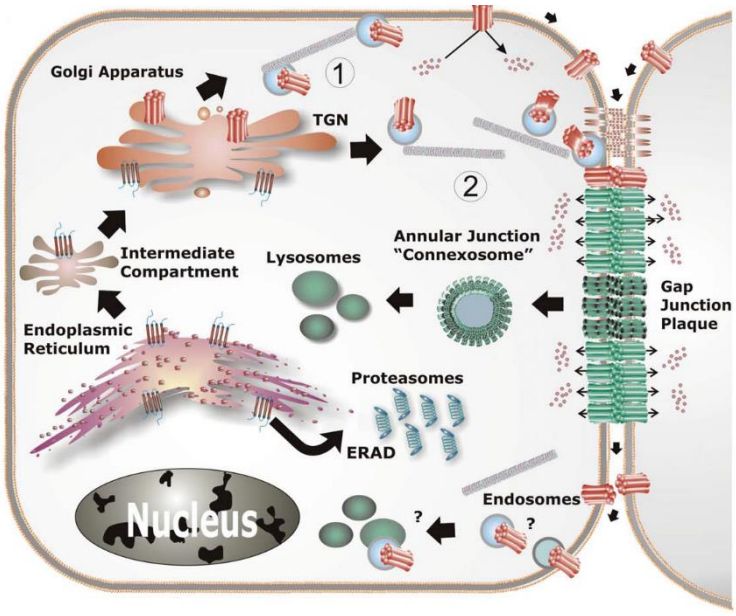

Figure 1.3. Connexin life cycle and turnover mechanisms. Trafficking of connexins to the plasma membrane follows secretory pathway and their degradation is done by either proteasomal or lysosomal pathways[9].

1.4. Connexins and Their Impact on Hereditary Human Diseases

Connexins are structural proteins of gap junctions and until know, studies showed that mutations on nine connexin isoforms are related with human hereditary disorders. Connexins that cause human hereditary diseases are Cx26, Cx30, Cx30.3, Cx31, Cx32, Cx43, Cx46, Cx47 and Cx50[37,38]. Mutations on Cx26, Cx30, Cx30.3 and Cx31 genes cause deafness and various skin disorders[39,40,41]. In addition, mutations on the Cx32 gene cause development of Charot- Marie- Tooth disease which is a neural disease and patients have distal muscle weakness and atrophy[42]. Mutations on Cx46 and Cx50 genes associated with cataract formation on eyes[43]. Furthermore, mutations on Cx47 gene are associated with Pelizaeus-Merzbacher-like disease (PMLD) which cause a central hypomyelinating[38].

Different types of mutations are determined on connexin genes. These mutations can be deletions, insertions, nonsense and missense mutations causing development of many human hereditary disorders. Mutations that abolish the function of connexins are called as loss of function mutations. On the other hand, missense mutations on connexin genes can also alter gene and protein function. These mutations are known as gain of function mutations[44]. Mutations on connexin genes affect protein structure and function.

Loss of function mutations prevent function of connexins and show different kind of blocking mechanisms for connexin function.

1.4.1. Loss of Function Mutations

There are five different mechanisms of loss of function mutations on connexin structure and function (Figure 1.4.1).

1) Truncation defects; insertion or deletion of nucleotide results in stop codon and premature termination of connexin synthesis occurs[45]. For example, 35delG in connexin 26 is the most frequent mutation in non-syndromic deafness in Caucasians and guanine deletion forms stop codon at the 13th position, resulting in truncated and non-functional protein[46] .
2) Trafficking defects and protein misfolding; nonsense, insertion and deletion mutations cause retention of proteins in the ER, the ER-Golgi intermediate compartment and the Golgi apparatus. Accumulation of proteins in organelles can be resulted from misolding and/or addition of post-translational motifs due to mutations. For instance, Cx26-D66H mutation associated with Vohwinkel syndrome and Cx26-R184Q mutation associated with non-syndromic deafness are examples for accumulation in Golgi apparatus[47,48].
3) Docking defects; gap junctions are formed by docking of two hemichannels and four hydrogen bonds formation is necessary between second extracellular loop interfaces on the plasma membrane for successful docking and gap junction formation[49]. Mutations at the docking sites can prevent gap junction formation and affect hemichannels function. Cx26-W172R and Cx32-N175D mutations are associated with non-syndromic deafness are the examples for docking defect[50,51].
4) Permeability and gating defects; in this case, mutations do not affect docking and gap junction plaques are formed with altered permeability. For instance, Cx26-V84L mutation has increased IP_3 permeability and cause non-syndromic deafness[52]. In addition, Cx46-D3Y and L11S mutations prevent passage of Ca^{2+} and Na^{+} and cause cataract formation on eyes[53].

5) Interactome defects; connexins have many interactome partners and these partners affect connexin trafficking and function[7]. Tubulin and calmodulin are the most searched partners until now. Cx43 interacts with tubulin for efficient cell surface localization. Cx43-fs230 mutation cause oculodentodigital dysplasia (ODDD) and diminish tubulin interaction. Therefore Cx43 accumulate in ER[54].

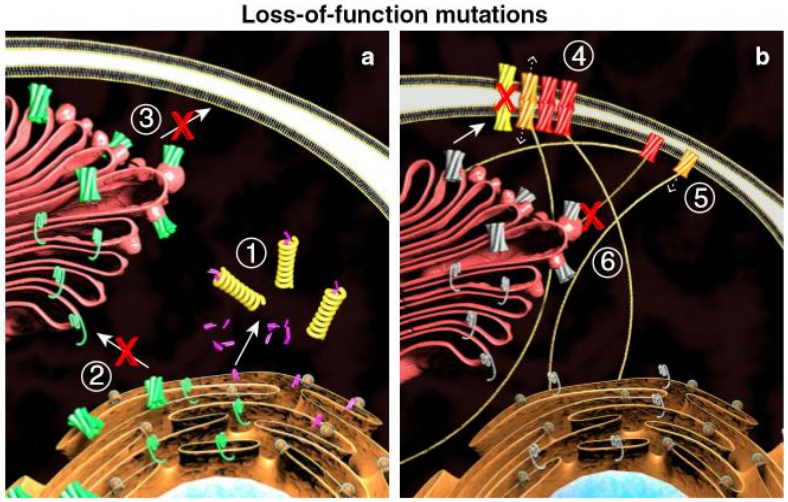

Figure 1.4.1. Loss of function mechanisms. 1) Truncation defects. 2) Trafficking defect. 3) Docking defect. 4) Permeability and gating defect. 5-6) Interactome defect[44].

1.4.2. Gain of Function Mutations

There are four different effects of gain of function mutations on connexin structure and function (Figure 1.4.2.).

1) Enhanced gap junction permeability; some gain of function mutations that result in increased gap junction permeability. Cx31-G12R mutation causes erythrokeratodermia variabilis and increases dye coupling between cells which indicated increase gap junction permeability[55]. This mutation is an example for this type of gain of function. However, there is less information about enhanced gap junction permeability causing mutations and further studies are necessary.
2) Enhanced hemichannel permeability; missense mutations increase permeability of hemichannels and cause depolarization of membrane and can

induce cell death[56]. Ca^{2+} deregulation and enhanced Ca^{2+} uptake into cell is the most frequent effect of enhanced hemichannel permeability. Cx26-G45E and Cx26-A40V missense mutations associated with KID syndrome form aberrant hemichannels and cause Ca^{2+} deregulation, damaging cell homeostasis[57].

3) Gain of interactome partners; in this mechanism, connexin mutants interact with proteins of which wild-type connexin normally do not interact with. Many Cx26 mutations such as Cx26-R75W causing palmoplantar keratoderma and D66H causing Vohvinkel syndrome interact with Cx43[58,48] but in normal situation, these two connexin isoforms do not oligomerize together[59].
4) Connexin half-life changes; connexins have half-life in range 1.5 to 5 hours. However, gain of function mutations can increase or decrease half-life of connexins. Cx43-G138R and G143S mutations that cause oculodentodigital dysplasia (ODDD) stay longer on the plasma membrane[60] and prolonged hemichannel or gap junction interaction enhance activity and induce cell death[61].

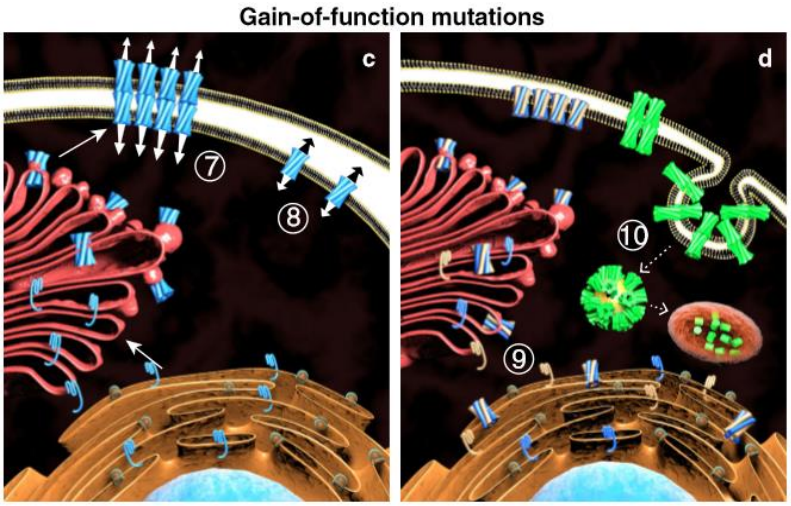

Figure 1.4.2. Gain of function mechanisms. 7) Enhanced gap junction permeability. 8) Enhanced hemichannel permeability. 9) Gain of interactome partners. 10) Connexin half-life changes[44].

1.5. Connexin 26 (Cx26) Mutations and Hearing Loss

Connexin 26 (Cx26) is the smallest connexin isoforms in human. Its molecular size is 26 kDa and it is highly expressed in the inner ear, the skin and cornea[6]. Cx26 is encoded by *GJB2* gene that is localized on chromosome 13q11-q12 region[19]. Mutations on the *GJB2* gene cause both non-syndromic and syndromic hearing loss in human (Figure 1.5)[62,3].

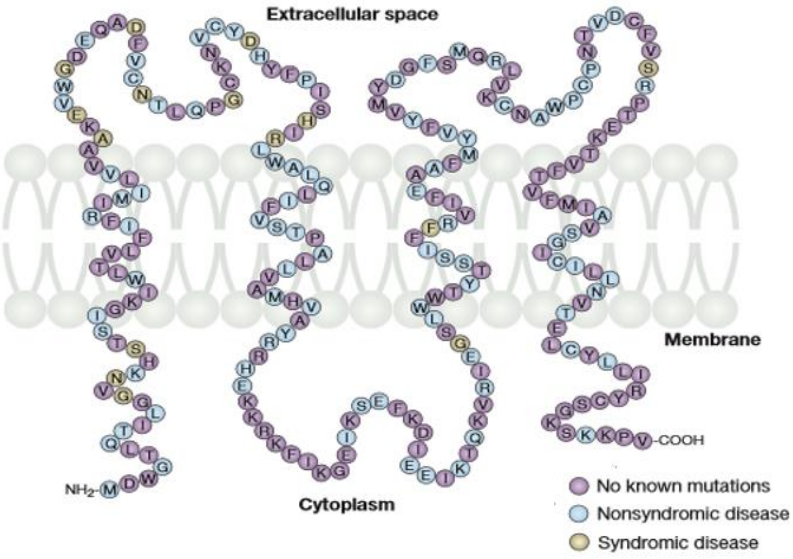

Figure 1.5. Amino acid sequence of Cx26 and determined mutation locations. Non-syndromic and syndromic deafness mutations are determined throughout the Cx26[3].

1.5.1. Non-syndromic Hearing Loss

50% of non-syndromic deafness is caused by mutations in the *GJB2* gene. Deletions, insertions, missense and nonsense mutations are determined on the *GJB2* gene causing non-syndromic deafness[63]. These mutations change sequence of *GJB2* gene and cause non-functional Cx26 synthesis[64]. Cx26 mutations causing non-syndromic hearing loss can be recessive and dominant[65]. 35delG single base deletion is the most frequent recessive Cx26 mutation observed in many populations in different frequencies[66]. Loss of function mutations on the *GJB2* gene is associated with non-

syndromic deafness. Truncation defect, protein folding defect, gating defect and docking defects are observed outcome of loss of function mutations in Cx26[44].

1.5.2. Syndromic Hearing Loss

Patients having syndromic hearing loss developed skin or eye problems besides deafness[37]. Syndromic deafness is autosomal dominant and connexin mutations associated with syndromic deafness are all single amino acid substitutions or deletions. There are different syndromic deafness disorders caused by connexin 26 mutations such as Vohwinkel syndrome (VS), Bart-Pumphrey syndrome (BPS), palmoplantar keratoderma (PPK) and keratitis- ichyhyosis deafness syndrome (KID)[67]. Enhanced hemichannel permeability and gain of interactome partners were determined as gain of function mechanisms for different Cx26 mutations[44].

1.5.2.1. Keratitis Ichthyosis Deafness (KID) Syndrome

Keratitis Ichthyosis Deafness (KID) syndrome is a rare congenital multisystem disorder. Until now, 100 cases are reported. It affects the epidermis (skin), cornea and the cochlea. It is inherited in autosomal dominant manner and mutations on the *GJB2* gene cause KID syndrome[68]. Phenotypes in KID syndrome can be severe with hyperkeratitis, nail dystrophy, loss of eyebrows and eyelashes, ichthyosis (fish-like skin), psoriasis and mucocutaneous infection[69]. In addition, patients with KID syndrome are under risk of developing benign and malignant cutaneous tumors[70].

Beside cochlea, the skin is the most affected organ on the human body due to KID syndrome. Skin is the largest and fastest growing organ in the human body and there are two layers in the skin[71]. Dermis is the location for appendages of the skin and the epidermis is the protective barrier layer. The epidermis is formed from the growth and the differentiation of keratinocyte that reside in four sublayers across the epidermis. These layers are stratum basale, stratum spinosum, stratum granulosum and stratum corneum from bottom to top. During differentiation, basal layer cells divide and after division, some part of basal layer cells stay in basal layer as stem cell precursor and other cells start to migrate and differentiate throughout the layers[72]. At the top, corneum

layer is formed from death cells. Moreover, differentiation cause changing in morphology and biochemical processes between all layers[73].

Keratinocytes express nine connexin isoforms and during cell division and differentiation, the expression pattern of connexin isoforms change. In basal layer, Cx26 and Cx43, in both spinosum and granulosum layers Cx30, Cx31, Cx31.1, Cx37, Cx40, Cx43 and 45, in granulosum, only Cx26 and Cx30.3 are highly expressed (Figure 1.4.2.2)[6]. Changes in connexin expression pattern throughout epidermis layers are associated with changing permeability properties of gap junctions. It was proposed that gap junctions coordinate keratinocyte differentiation by differential connexin expression[74,75,76]. On the other hand, Ca^{2+} homeostasis is another important factor during differentiation of keratinocytes. There is a Ca^{2+} gradient which is the lowest concentration at basal layer and the highest concentration at granulosum layer. This Ca^{2+} gradient enhances expression of proteins that promote keratinocytes differentiation. Connexins are thought to have roles in maintenance of Ca^{2+} gradient and mutant connexins can distrupt the gradient and prevent proper differentiation[56].

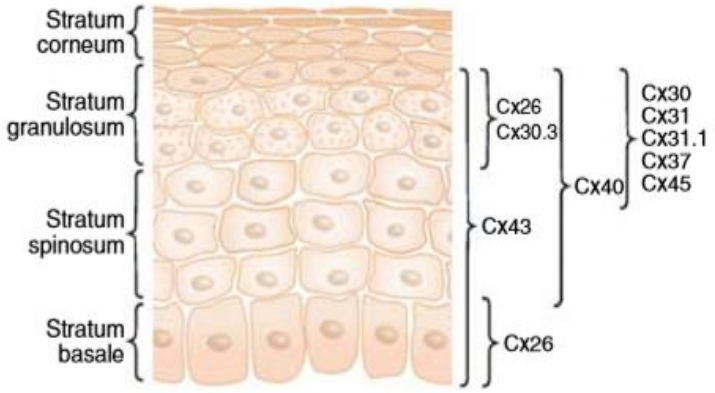

Figure 1.5.2.2. Sublayers of epidermis and expressed connexin isoforms in each layer. These layers are Stratum basale, Stratum spinosum, Stratum granulosum and Stratum corneum[6].

Missense mutations on the *GJB2* gene associated with KID syndrome are usually observed between N-terminal to first extracellular loop (EC1) that are responsible for voltage gating and hemichannel docking, respectively[3,77]. However, mutations can also be observed in other domains such as Cx26-A88V mutation on TM2 domain[78]. Characterization of KID syndrome associated Cx26 mutations by using various methodologies including western blot, dye uptake assays, internal Ca^{2+} content

measurement, ATP relese assay, electrophysiological hemichannel current measurement and whole cell voltage procedures enabled the understanding of effecta of Cx26 mutations on protein and channel function[79,80] . G12R, N14Y and D50N mutations were shown to have aberrant hemichannel functionality[81,77]. In addition, Cx26-G45E and A40V mutations showed increased hemichannel activity and result in cell death [62]. Moreover, Cx26-A88V and D50A showed increased hemichannels functionality and Cx26-A88V caused cell death while Cx26-D50A did not[80]. Aberrant hemichannel formation can change the permeability of hemichannels. Permeability of Ca^{2+} and ATP is changed and internal Ca^{2+} amount increase and ATP is released from the cells. These two changes can affect cell physiology and can play role in cell death[82,83]. On other hand, Cx26-S17F missense mutation did not form gap junction channels or hemichannels but altered epidermal differentiation in KID syndrome mouse models[84]. Characterized missense mutations associated with KID syndrome showed that each can affect Cx26 structure and function differently. Therefore, each mutation should be individually characterized to understand their effect on Cx26 and its relation with KID syndrome.

1.6. Aim of the Project

In a previous study from our laboratory[85] , dye uptake studies showed that cells with Cx26-I30N and D50Y mutations had increased ethidium bromide and neurobiotin uptake in cells compared to Cx26-WT containing cells, suggesting the formation of aberrant hemichannels on the plasma membrane in N2A and HeLa cell lines (Figure 1.6). However, effects of mutations on hemichannel functionality such as their effect on Ca^{2+} content, ATP release and interaction with other connexins (Cx43) has not been investigated. Therefore, in this project, we aimed to decipher functions of aberrant hemichannels formed by Cx26-I30N and D50Y mutations in N2A, HeLa and immortalized keratinocyte cell line HaCaT.

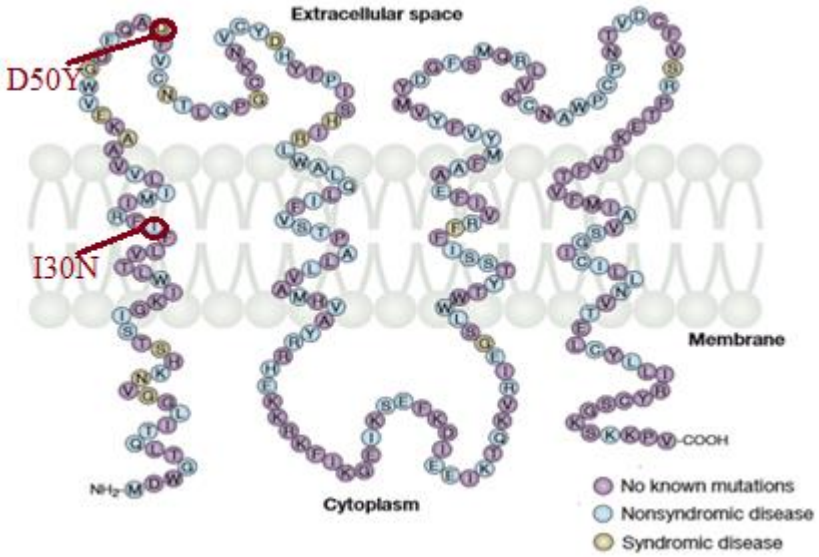

Figure 1.6: Location of Cx26-I30N and D50Y mutations on Cx26 [3].

CHAPTER 2

MATERIALS & METHODS

2.1. DNA Constructs and Chemical Transfection

Cx26-WT, I30N and D50Y cDNAs were cloned into pCS2+ and pIRES2EGFP2 expression vectors. Midiprep DNA isolation was performed with Invitrogen DNA isolation kit following the manufacturer's protocol (Cat# K210015). Cells were transfected with different transfection reagents and were used 24 h after transfection. Lipofectamine 2000 (Invitrogen, Cat# 11668-027) transfection reagent was used for human cervical cancer cells (HeLa), mouse neuroblastoma (N2A) and Lipofectamine 3000 (Invitrogen, Cat# L3000008) was used for human keratinocyte (HaCaT) cell lines.

Lipofectamine 2000 was used in 3µl DNA: 6µl reagent ratio. Trasfection was performed by following the manufacturer's protocol. In short, two eppendorfs were prepared,one for DNA and one for Lipofectamine 2000. Then, 100 µl serum free DMEM was added in Eppendorf tubes. DNA and Lipofectamine 2000 were added on DMEM in 3 µg and 6µl, respectively and mixed without pipetting. After 5 mins incubation at room temperature (RT), DMEM including DNA and Lipofectamine 2000 were mixed and incubated for 20 mins at RT. Finally, suspension was added on cells drop by drop and 3.2 µM $CaCl_2$ was added on cells. Moreover, transfection with Lipofectamine 3000 was performed by following the manufacturer's protocol. Firstly, two eppendorfs were prepared for DNA and Lipofectamine 3000. 125 µL Opti-MEM was added in Eppendorf tubes and DNA (2µg) and Lipofectamine 3000 (6µl) were added on DMEM and mixed without pipetting. After mixing DNA and Lipofectamine 3000 suspention in an Eppendorf tube, suspension was incubated for 10 mins at RT. Finally, suspension was added on cells drop by drop and 3.2 µM $CaCl_2$ was added on cells.

2.2. Maintenance of N2A, HeLa and HaCaT Cell Lines

N2A, HeLa and HaCaT cells were used to perform experiments. N2A cells were grown in high glucose Dulbecco's Modified Eagle Medium (DMEM) (GIBCO, Cat# 41966-029) supplemented with 10% Fetal Bovine Serum (FBS) (Biological Industries, Cat# SH30243.01) and 1% penicillin streptomycin (Invitrogen, Cat# 1092595). N2A cells were cultured in tissue treated plates and re-plated by incubating with 0.25% Trypsin/EDTA solution (BI, Cat# 03-052-1B) for 5 min. N2A cells were incubated in 5% CO_2 and 37^{o}C conditions.

HeLa cells were grown in low glucose DMEM (GIBCO, Cat# 311885-023) supplemented with 10% (FBS) and 1% penicillin streptomycin. Cells were cultured in tissue culture treated plates and incubated on 5% CO_2 and 37^{o}C conditions. 0.25% Trypsin/EDTA solution was used for re-plating of cells and incubated 5 min at 37^{o}C.

HaCaT cells were grown in high glucose DMEM supplemented with 10% FBS and 1% penicillin streptomycin. HaCaT was lifted off by first incubating with EDTA (BI, Cat# 03-015-1B) for 20 min and then, 0.05% Trypsin/EDTA (BI, Cat# 03-053-1B) for 2 min at 5% CO_2 and 37^{o}C incubator. HaCaT cells were incubated in 5% CO_2 and 37^{o}C conditions.

2.3. Immunostaining and Fluorescence Imaging

For immunostaining experiments, HeLa ($3x10^5$) and HaCaT ($4x10^5$) cells plated on glass coverslips were transfected with pCS2+Cx26-WT and mutant gene constructs using Lipofectamine 2000 and Lipofectamine 3000, respectively. First of all, cells were washed with 1X Phosphate Buffer Saline (PBS) twice (BI, Cat# 02-023-5A) and fixed with 4% Paraformaldehyde (PFA) for 20 min at room temperature (RT). Cells were permeabilized with 0.1% Triton X-100/ 1X PBS for 15 min at RT. Then, blocking was performed with 5% bovine serum albumin (BSA) in 0.1% Triton X-100/ 1X PBS for 1h at RT with shaking at 60 rpm. Later, cells were incubated with a 1:500 dilution of polyclonal rabbit anti-Cx26 primary antibody (Invitrogen, Cat# 51-2800) for 1h at RT temperature. Cells were washed with 1X PBS three times and then cells were incubated with a 1:200 dilution of Phalloidin 488 (Invitrogen, Cat# A22287), Alexa555-

conjugated goat anti-rabbit secondary antibody (Invitrogen, Cat# A21428) and DAPI (1:200) (Sigma, Cat# D95242-10MG) for 45 mins at RT. Finally, cells were washed with 1X PBS and dH2O and mounted on microscope slides and covered with nail polish to prevent drying. Images were taken under the fluorescence microscope (IX83 Olmypus, Japan) with X 40 and X 100 magnification and merged on the cellSens software and ImageJ (NIH) software.

2.4. Co-immunostaining and Fluorescence Imaging

HeLa ($3x10^5$) and HaCaT ($4x10^5$) cell lines were grown on cover slips and transfected with pCS2+Cx26 constructs using Lipofectamine 2000 and Lipofectamine 3000, respectively. 24 h after transfection, cells were washed with 1X PBS twice and fixed with 4% (PFA) for 20 min at RT. Cells were permeabilized with 0.1% Triton X-100/ 1X PBS for 15 min at RT. Then, blocking was performed with 5% BSA in 0.1% Triton X-100/ 1X PBS for 1h at RT with shaking at 60 rpm. For Cx26-Golgi apparatus staining, cells were incubated with a 1:500 dilution of polyclonal rabbit anti-Cx26 primary antibody and monoclonal mouse golgin-97 primary antibody (Invitrogen, Cat# A-21270) for 1h at RT. After cells were washed with 1X PBS three times, they were incubated with a 1:200 dilution of Alexa555-conjugated goat anti-rabbit secondary antibody (Invitrogen, Cat# A21428), Alexa488-conjugated goat anti-mouse secondary antibody (Invitrogen, Cat# A11017) and DAPI for 45 min at RT. In final step, cells were washed with PBS for 10 min three times at RT and rinsed with dH2O and dried. Cover slips were mounted on microscope slides and covered with nail polish to prevent drying. Images were taken under fluorescence microscope (IX83 Olmypus, Japan) with X 40 and X 100 magnification and merged on the Olympus cellSens Software and ImageJ (NIH) software.

2.5. Semi-quantitative RT-PCR and Gene Expression Analysis

N2A ($5x10^5$) and HaCaT ($4x10^5$) cells were transfected with pIRES2EGFP2Cx26-WT and mutant constructs as explained in Section 2.1. 24 h after transfection, cells were washed with 1X PBS two times and flash frozen with liquid nitrogen and plates were stored in -80^{o}C.

2.5.1. RNA Isolation

Total RNA isolation from frozen plates was done with RNA isolation kit (Invitrogen, Cat# AM1910) following manufacturer's protocol. First of all, cells were lyzed with lysis buffer for 5 min and collected in 1.5 ml eppendorf tubes. Cell suspension was homogenized with 1 ml insulin syringe for 5 times to prevent viscosity. Then, 70% ethanol was added and suspention was loaded on column. After washing columns with wash buffer, columns were incubated with DNase (Invitrogen, Cat# 18068-015) for 15 min at RT. After, washing columns with wash buffer twice, RNA was eluted with RNase free water. Purity and concentration of RNA samples were measured by Nanodrop (ND-1000 Spectrophotometer).

2.5.2. cDNA Synthesis

cDNA synthesis from total RNA was performed with Fermentas First Strand cDNA Synthesis Kit (Thermo, Cat# K1622) using 1µg/µl total RNA. First of all, RNA and random primer suspension was incubated at 65^{o}C for 5 min. Then, master mix was prepared, including reaction buffer, dNTPs, ribolock RNase inhibitor and reverse transcriptase and mixed with RNA suspension. Reaction was done in PCR machine using, 25^{o}C for 5 min, 42^{o}C for 1 h and 70^{o}C for 5 min cycles (Applied Biosystems, Veriti Thermal Cycler).

2.5.3. Semi-quantitative RT-PCR

SYBR Green based qRT-PCR was done in Biorad IQ5 Thermal Cycler. Primers (Table 2.6.1), SYBR Green and cDNA suspension was loaded on 96 well plates and reaction was done in qRT-PCR machine using 98^{o}C for 5 min, 95^{o}C for 30 sec, 60^{o}C for 30 sec and 72^{o}C for 10 min cycles. Results were analyzed by Delta-Delta Ct method. GAPDH was used as a housekeeping control.

Table 2.5.3. Forward and reverse primer sequences used in qRT-PCR.

Gene	**Forward Primer (5' to 3')**	**Reverse Primer (5' to 3')**
Human_Cx26	ctgcagctgatcttcgtgtc	aagcagtccacagtgttg
Human_Cx43	gtgcctgaacttgccttttc	ccctcccagcagttgagtagg
Human_GAPDH	gaaggtgaaggtcggagtca	aatgaaggggtcattgatgg
Mouse_GAPDH	gacatgccgcctggagaaac	agcccaggatgccctttagt
EGFP	acgtaaacggccacaagttc	aagtcgtgctgcttcatgtg

2.6. Western Blot

Total protein isolation and concentration measurement of isolated protein by Bradford assay were performed as explained in Sec 2.6. Equal amounts of protein for each sample was incubated with 5X SDS loading buffer (250 mM Tris-HCI, 10% SDS, 30% Glycerol, 5% β-mercaptoethanol, 0,02% Bromophenol Blue) at 95^{o}C for 5 min. Samples were loaded on 15% SDS-polyacrylamide gel, run at 20mA for 3 h. After, proteins were transferred from SDS- polyacrylamide gel to nitrocellulose membrane at 250 mA for 2 hours and blocked with 5% powder milk for 1 h at RT. Then, nitrocellulose membrane was incubated with a 1:500 dilution of polyclonal rabbit anti-Cx26 primary antibody at +4 ^{o}C overnight by shaking. Following day, membranes were washed with 1X Tris-Buffered Saline and Tween 20 (TBS-T) three times for 10 min. Then, membrane was incubated with a 1:2500 dilution of peroxidase conjugated goat anti-rabbit secondary antibody (Pierce, Cat# 31460) for 2h at RT and washed with 1X TBS-T three times for 10 min. For visualization of proteins, SuperSignal West Pico Chemiluminescent Substrate (Thermo, Cat# 34080) and Versadoc imaging system (Biorad, IZTECH Biomer, İzmir, Turkey) was used. Gamma (γ) tubulin was used as a loading control in western blot assays. Membrane was incubated with a 1:10,000

dilution of monoclonal mouse anti-γ–tubulin primary antibody (Sigma, Cat# T6557) for 2 h at RT and incubated with a 1:1000 dilution of monoclonal goat anti-mouse secondary antibody (Dako, Cat# 00071312) for 2h at RT. After visualization process was completed and normalization was done with protein band of γ tubulin.

2.7. Internal Ca^{2+} Content Measurement

Flow cytometry was used for the measurement of internal Ca^{2+} content with Fluo-3AM (Invitrogen, Cat# F-1241) Ca^{2+} indicator[84]. N2A ($5x10^5$) and HaCaT cells ($4x10^5$) were plated onto 6 well plates and transfected with pCS2+Cx26-WT and mutant clones. 24 h after transfection, cells were washed with Ca^{2+} free PBS twice for 5 min and incubated with 5μM Fluo-3AM at 37°C for 30 min. Then, cells were washed with PBS, trypsinized with 0.25% Trypsin/EDTA solution for N2A and 0.05% Trypsin/EDTA for HaCaT. Then, cells were resuspended in 300 μl Hank's Balanced Salt Solution (HBSS). Fluo-3AM signal intensity was detected with flow cytometry (BD FACSCANTO, IZTECH Biomer, İzmir, Turkey).

2.8. ATP Release Assay

ATP release experiments were done by using ATP determination kit (Invitrogen, Cat# A22066) following manufacturer's protocol. N2A ($5x10^5$) and HaCaT ($4x10^5$) cells were transfected with pCS2+Cx26-WT and mutant constructs as explained in Section 2.1. 24 h after transfection, cells were washed and incubated with 1X PBS without calcium for 4 hours at 37°C. Then cells were incubated with 1X PBS for 15 min at 37°C and PBS was collected and flash frozen with liquid nitrogen. Six ATP standards (50pM, 100pM, 200pM, 500pM, 1000pM and 4000pM) were prepared to plot a standard curve. Luminometric measurement of ATP standards and samples were done in Thermo Varioskan Flash Multimode Reader and released ATP concentrations of samples were calculated by using the standard curve.

ATP concentrations were compared by normalizing them to total protein amounts. Total protein isolation from N2A and HaCaT cells was performed after freezing cells with liquid nitrogen. First, cells were lysed in Lysis buffer including

10mmol/L Tris pH 7.5, 1 mmol/L Ethylenediaminetetraacetic acid (EDTA), 0.1 % Triton X-100, 1X Protease inhibitor (PI) and 1 mM Dithiothreitol (DTT) and scraped with cell lifter for 5 min. Then, the cell suspension was homogenized with 1 ml insulin syringe for 5 times and incubated on ice for 20 min. Finally, the cell suspension was centrifuged at 14,000 rpm, at +4^{o}C for 30 min and supernatant of mixture including total proteins was collected in 1.5 ml Eppendorf tubes and stored at -80^{o}C. Protein concentration was measured with Bradford assay. Protein and Bradford reagent were mixed in 1:40 ratio, respectively and samples were measured in Thermo GeneSYS 10S VIS spectrophotometer at 595 nm. BSA was used for standard curve formation from 0.5µg/ml to 8µg/ml range and protein concentrations were calculated using the standard curve.

2.9. Cell Size Measurement

N2A ($5x10^5$) and HaCaT ($4x10^5$) cells were transfected with pIRES2EGFP2Cx26-WT, I30N and D50Y constructs as explained in Section 2.1. Cell size was measured using flow cytometry and average of FSC values of GFP positive cells was used as a measure of relative cell size.

2.10. Apoptosis Assay

N2A ($5x10^5$) and HaCaT ($4x10^5$) cells were transfected with pIRES2EGFP2Cx26-WT, I30N, D50Y constructs as explained in Section 2.1. Apoptosis assay was performed with Annexin V-PE Apoptosis Detection Kit (Abcam, Cat# ab14155) following manufacturer's protocol. 24 h after transfection, cells were washed with 1X PBS twice. 5 µl Annexin V and 7-AAD was mixed with 500 µl 1X binding buffer for one well. Then, mixture was put on cells and incubated for 15 min at RT in dark. After, cells were washed with 1X PBS, trypsinized and resuspended in 300µl 1X binding buffer. In final step, apoptotic and necrotic cells were analyzed by flow cytometry.

2.11. Colocalization Analysis

Colocalization analysis was performed by using Fiji Coloc 2 plug-in. Costes' colocalization coefficient was used in this study to determine colocalization between channels. First of all, pixels of green and red channels were calculated for Pearson's correlation. Then, pixels of two channels are randomized 200 times and results were compared with Pearson's correlation results. If original Pearson's correlation was higher than 95%, it was accepted as significant colocalization[86].

2.12. Statistical Analysis

All results were expressed as mean (± standard deviation). Two tailed unpaired t-test was applied to graphs to determine the significance in results. P-values lower than 0.05 were accepted as a significant difference. Kruskal-Wallis rank sum test followed by Mann-Whitney test was applied for colocalization analysis and statistical significance was accepted as $p < 0.05$.

CHAPTER 3

RESULTS

3.1. Cellular Localization of Cx26-I30N and D50Y Mutations in HeLa Cells

Immunostaining of HeLa cells were performed to observe cellular localization of Cx26-I30N and Cx26-D50Y mutant proteins in cells. HeLa contain negligible amount of Cx45[87] that do not interact with Cx26 therefore we could observe the direct effect of mutations on gap junction formation and localization in these cells. In previous studies, it was indicated that KID syndrome associated Cx26 mutations were unable to form gap junction but can form leaky hemichannels[62,3]. Therefore, we wanted to determine the cellular localization and gap junction formation of Cx26-I30N and D50Y mutations in HeLa cells.

Result of immunostaining experiments showed that HeLa cells transfected with Cx26-I30N and D50Y constructs could synthesize Cx26 (Figure 3.1 (Red signal)). In addition, Cx26-I30N and D50Y mutant proteins mainly localized to cytoplasm near nucleus (Figure 3.1 B and C (white arrows)), while Cx26-WT localized on plasma membrane where they formed gap junction plaques between adjacent cells (Figure 3.1 A, white arrow). However, Cx26-I30N and D50Y mutants were unable to form gap junction plaque on the contact site of adjacent cells. Protein localization was observed mainly in cytoplasm (Figure 3.1 B,C, white arrows)

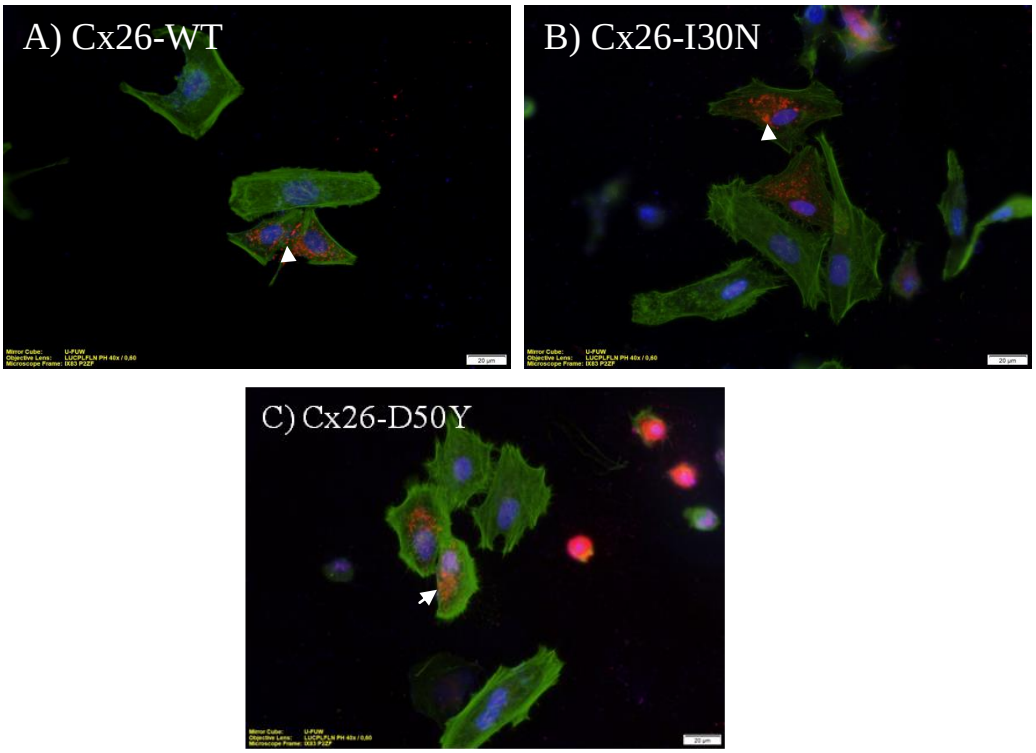

Figure 3.1. Immunostaining of transfected HeLa cells. Images were taken under fluorescence microscope with X 40magnification (scale bar: 20µm). A) pCS2+Cx26-WT formed gap junction plaques (white arrow). B) pCS2+Cx26-I30N C) pCS2+Cx26-D50Y. Red color represents Cx26 localization, green color represents actin being used for visualization of cell borders and blue color represents nucleus.

3.2. Cellular Localization of Cx26-I30N and D50Y Mutations in HaCaT Cells

Immunostaining of HaCaT cells were performed to observe localization and gap junction formation of Cx26-I30N and D50Y mutations in the presence of other connexin isoforms. HaCaT cell line was specifically chosen because I30N and D50Y mutations were obtained in KID syndrome patients and effect of mutations on human keratinocytes should be observed to understand their role in KID syndrome development[88]. In HeLa cells, immunostaining results indicated that Cx26-I30N and D50Y mutants were unable to form gap junction plaque while it can change in HaCaT cells because they express other connexin isoforms such as Cx31 and Cx43[89,90]. Connexins interact with each other and form heteromeric hemichannels and heterotypic gap junctions[91]. With this perspective, we aimed to investigate localization and gap junction formation of Cx26-I30N and D50Y in HaCaT cells.

Results of HaCaT immunostaining showed that HaCaT cells transfected with Cx26-I30N and D50Y construct synthesized Cx26 (Figure 3.2 (Red signal)) and localized mainly in cytoplasm near nucleus and cannot form gap junction plaque while cells with Cx26-WT could form gap junction plaque (Figure 3.2 A (white arrow)). HaCaT immunostaining indicated that other connexins such as Cx43 did not affect the localization of I30N and D50Y mutations and/or the formation of gap junctions. As in HeLa cells, mutant proteins are mainly localized in cytoplasm (Figure 3.2 B,C, white arrows).

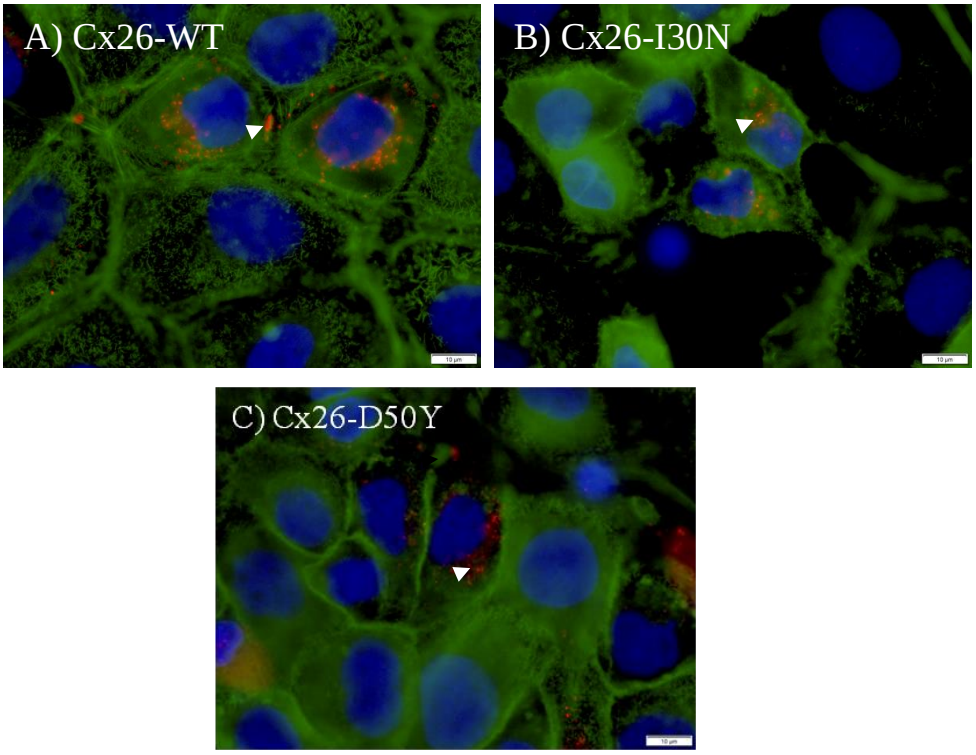

Figure 3.2. Immunostaining of transfected HaCaT cells. Images were taken under fluorescence microscope with X 100 magnification (scale bar: 10µm). A) pCS2+Cx26-WT indicated gap junction plaque formation B) pCS2+Cx26-I30N C) pCS2+Cx26-D50Y. Red color indicates Cx26, green color indicates actin and blue color indicates nucleus staining.

3.3. Endoplasmic Reticulum (ER) Accumulation of Cx26-I30N and D50Y Mutations in HeLa Cells

Cx26 and ER co-immunostaining was performed to observe ER localization of Cx26-I30N and D50Y mutant proteins in HeLa cells. Mutant Cx26 protein can localize organelles because their trafficking to plasma membrane is mediated by secretory pathway[27]. As immunostaining experiments showed that Cx26-I30N and D50Y

mutations mostly localize in cytoplasm. We aimed to investigate ER localization of Cx26-I30N and D50Y proteins.

Result of co-immunostaining showed that Cx26-I30N and D50Y mutant proteins did not localized in ER (Figure 3.3). There was no difference between Cx26-WT and mutant protein signals. Colocalization was manifested by yellow color. However, yellow color was equally observed between Cx26-WT and mutant proteins. Observation of yellow color in all conditions were expected since during trafficking connexin proteins pass through the ER.

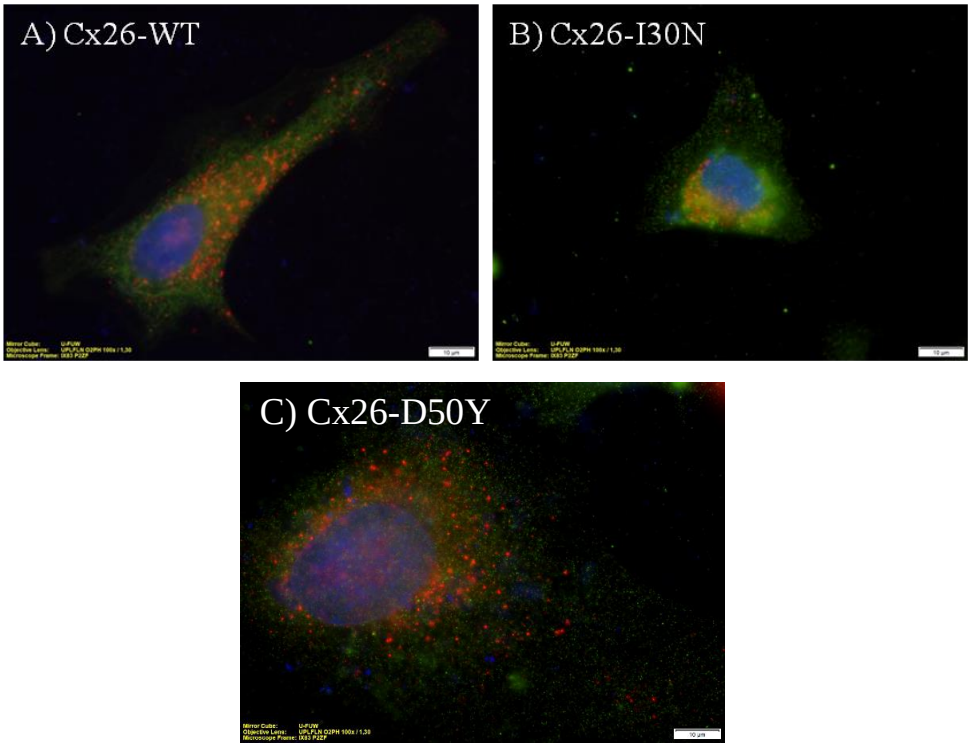

Figure 3.3. Cx26-ER co-immunostaining of transfected HeLa cells. Images were taken under fluorescence microscope with X 100 magnification (scale bar: 10µm) A) pCS2+Cx26-WT B) pCS2+Cx26-I30N C) pCS2+Cx26-D50Y. Red color indicates Cx26, green color indicates ER and blue color indicates nucleus staining. Colocalization of Cx26 on ER indicated as yellow color.

3.4. Golgi Apparatus Accumulation of Cx26-I30N and D50Y Mutations in HeLa Cells

Golgi apparatus co-immunostaining was performed in HeLa cells to observe the effect of Cx26-I30N and D50Y mutations on Cx26 trafficking. In immunostaining results of HeLa cells, Cx26-I30N and Cx26-D50Y mutants localized near the nucleus

and we suspected their accumulation in the Golgi apparatus. Therefore, related with HeLa immunostaining results, we aimed to observe Golgi apparatus accumulation of Cx26-I30N and D50Y mutants.

Results of Cx26-Golgi apparatus co-immunostaining in HeLa cells indicated that Cx26-I30N and D50Y mutants colocalized in Golgi apparatus while Cx26-WT did not (Figure 3.4). Costes correlation coefficient was calculated for colocalization analysis and correlation between images which was more than 95% was accepted as significant. 95% or higher correlation indicated that localization of Cx26 in the Golgi apparatus. 2 of 25 (8%) Cx26-WT, 19 of 33 (58%) Cx26-I30N and 13 of 26 Cx26-D50Y images indicated significant colocalization. Colocalization ratio differences are significantly higher ($p<0.01$) in both Cx26-I30N and D50Y when compared with WT.

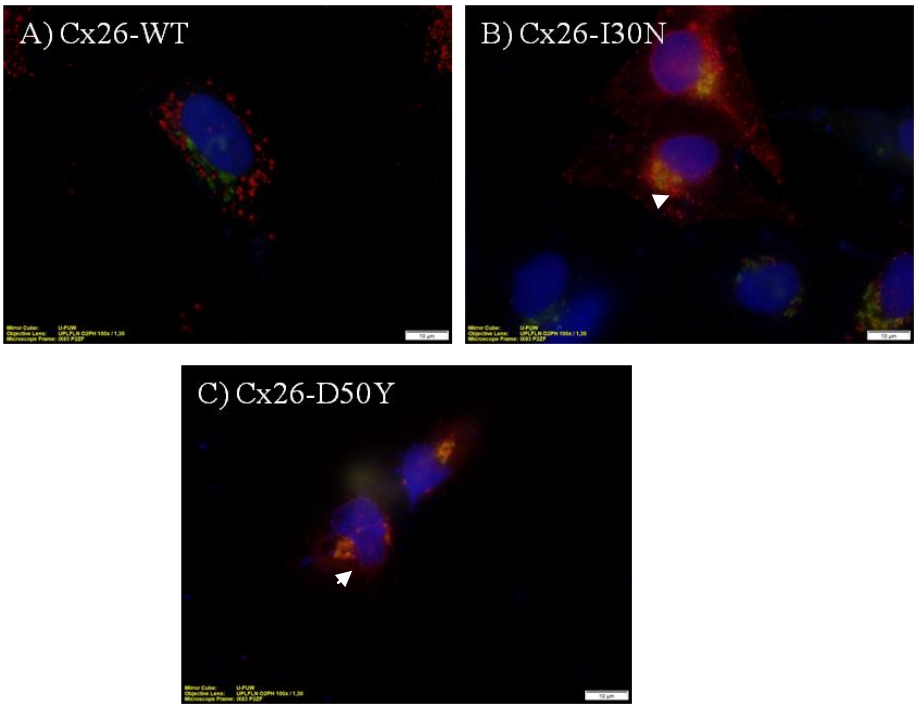

Figure 3.4. Cx26-Golgi apparatus co-immunostaining of transfected HeLa cells. Images were taken under fluorescence microscope with X 100 magnification (scale bar: 10μm) A) pCS2+Cx26-WT B) pCS2+Cx26-I30N C) pCS2+Cx26-D50Y. Red color indicates Cx26, green color indicates Golgi apparatus and blue color indicates nucleus staining. Colocalization of Cx26 on Golgi apparatus indicated as yellow color.

3.5. Golgi Apparatus Accumulation of Cx26-I30N and D50Y Mutations in HaCaT Cells

After observing Golgi accumulation of Cx26-I30N and D50Y mutants in HeLa cells, same experiment was performed with HaCaT cells to examine effect of Cx26-I30N and D50Y mutations on Cx26 trafficking. Merged images of co-immunostaining results showed that Cx26-I30N and Cx26-D50Y mutant colocalize in Golgi apparatus (Figure 3.5 B and C (yellow color)) while there was no colocalization in WT condition (Figure 3.5 A). Colocalization analysis indicated that only 3 of 18 images of Cx26-WT transfected cells (16%) had significant Costes correlation coefficient result (>95%) whereas for Cx26-I30N, 11 of 18 (61%) images and for Cx26-D50Y, 10 of 15 (67%) images had significant colocalization (Figure 3.5 B and C (white arrows)). Statistical analysis showed that there were Golgi apparatus accumulation of Cx26-I30N and D50Y mutant proteins ($p < 0.01$) in HaCaTs.

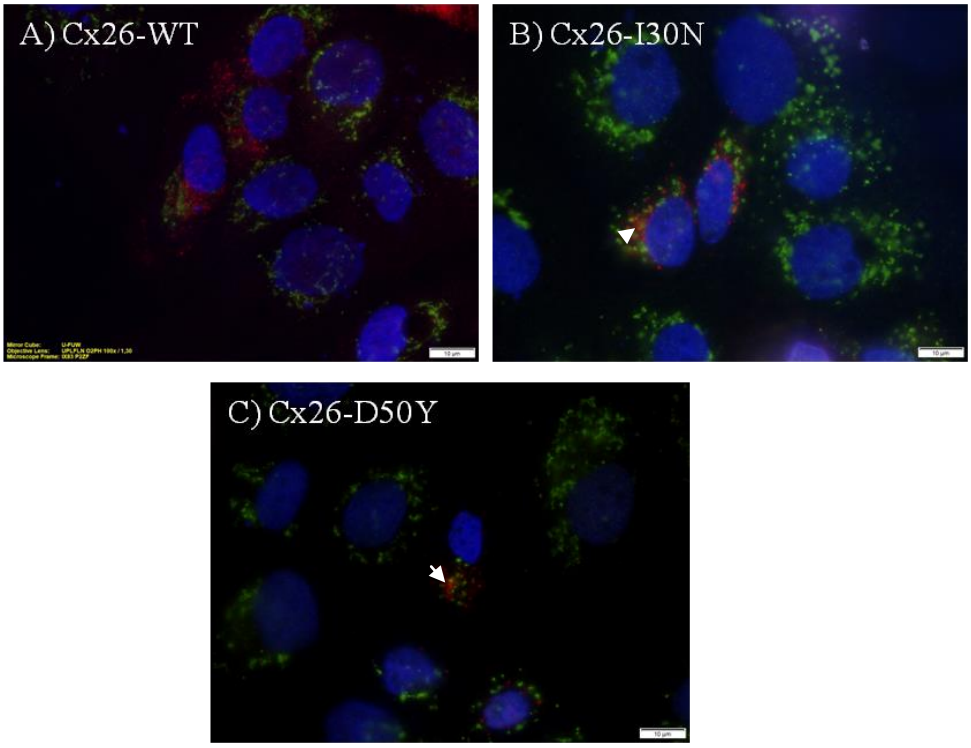

Figure 3.5. Cx26-Golgi apparatus co-immunostaining of transfected HaCaT cells. Images were taken under fluorescence microscope with X 100 magnification (scale bar: 10μm) A) pCS2+Cx26-WT B) pCS2+Cx26-I30N C) pCS2+Cx26-D50Y. Red color indicates Cx26, green color indicates Golgi apparatus and blue color indicates nucleus staining. Colocalization of Cx26 on Golgi apparatus indicated as yellow color.

3.6. mRNA Level of Cx26 and Cx43 in HaCaT Cells

mRNA expression profile of Cx26 and Cx43 was determined in HaCaT cells to understand effect of Cx26-I30N and D50Y mutations on expression of Cx26 and endogenous Cx43 genes. Results of semi quantitative RT-PCR showed that mRNA expression of Cx26-I30N and D50Y were slightly decreased when compared with mRNA expression level of Cx26-WT (Figure 3.6 A). Decreased mRNA level of Cx26-I30N was statistically significant ($p < 0.05$). Moreover, endogenous Cx43 expression level was investigated to observe effect of Cx26-I30N and D50Y mutations on Cx43 expression. Semi-quantitative RT-PCR result of Cx43 gene showed that its expression elevated by 1.2 fold when co-expressed with Cx26-I30N and D50Y mutations (Figure 3.6 B). This elevation of Cx43 gene expression was statistically significant ($p < 0.01$). Semi-quantitative RT-PCR result of Cx43 gene showed that Cx26-I30N and D50Y mutations increased Cx43 gene expression.

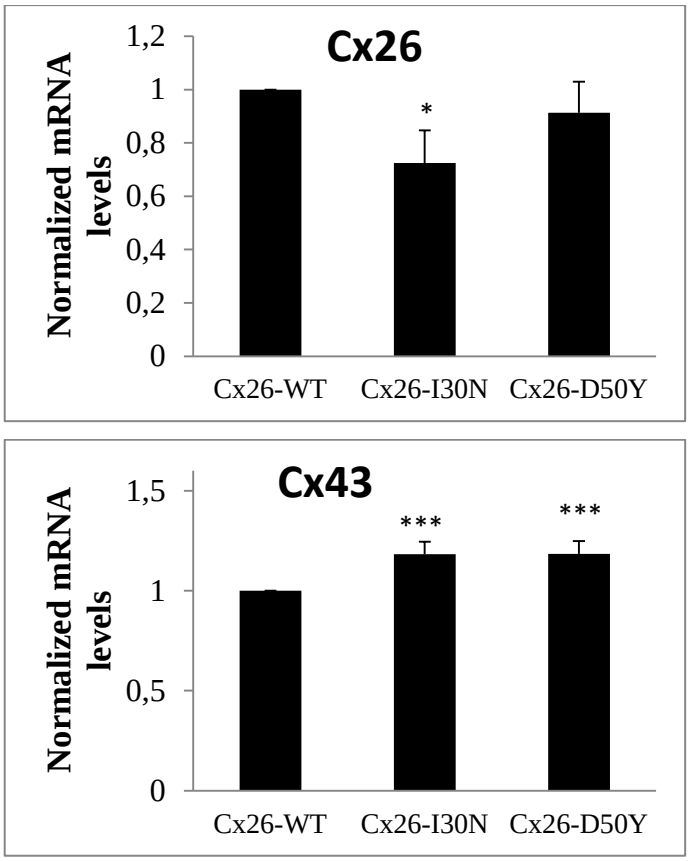

Figure 3.6. mRNA expression profile of transfected HaCaT cells for Cx26 and Cx43 genes. GAPDH was used as housekeeping gene and normalization was done with EGFP. A) Graph indicates normalized Cx26 mRNA expression level in HaCaT cells ($p<0.05$ *). B) Graph indicates normalized Cx43 mRNA expression level in HaCaT cells ($p< 0.01$ ***).

3.7. Protein Level of Cx26-I30N and D50Y Mutants

After examination of mRNA levels of Cx26 and Cx43, we performed western blot to observe protein levels of Cx26-I30N and D50Y mutants in N2A and HaCaT cells. In mRNA level, Cx26-I30N mutation decreased *GJB2* gene expression. Decreased mRNA level can affect level of Cx26-I30N and D50Y mutant proteins. Therefore, we aimed to observe effect of Cx26-I30N and D50Y mutations on protein synthesis of Cx26 gene. Western blot results indicated that protein amount of Cx26-D50Y decrease by three fold in N2A and two fold in HaCaT cells when compared with protein amount of WT (Figure 3.7 B). During western blot experiments, we were unable to detect Cx26-I30N protein band while we could observe mRNA expression and protein localization on immunostaining experiments. In addition, pIRES2EGFP and pCS2+ expression

vectors were used as negative controls in N2A and HaCaT cells, respectively. No Cx26 protein synthesis was detected in negative controls (Figure 3.7 A)

.

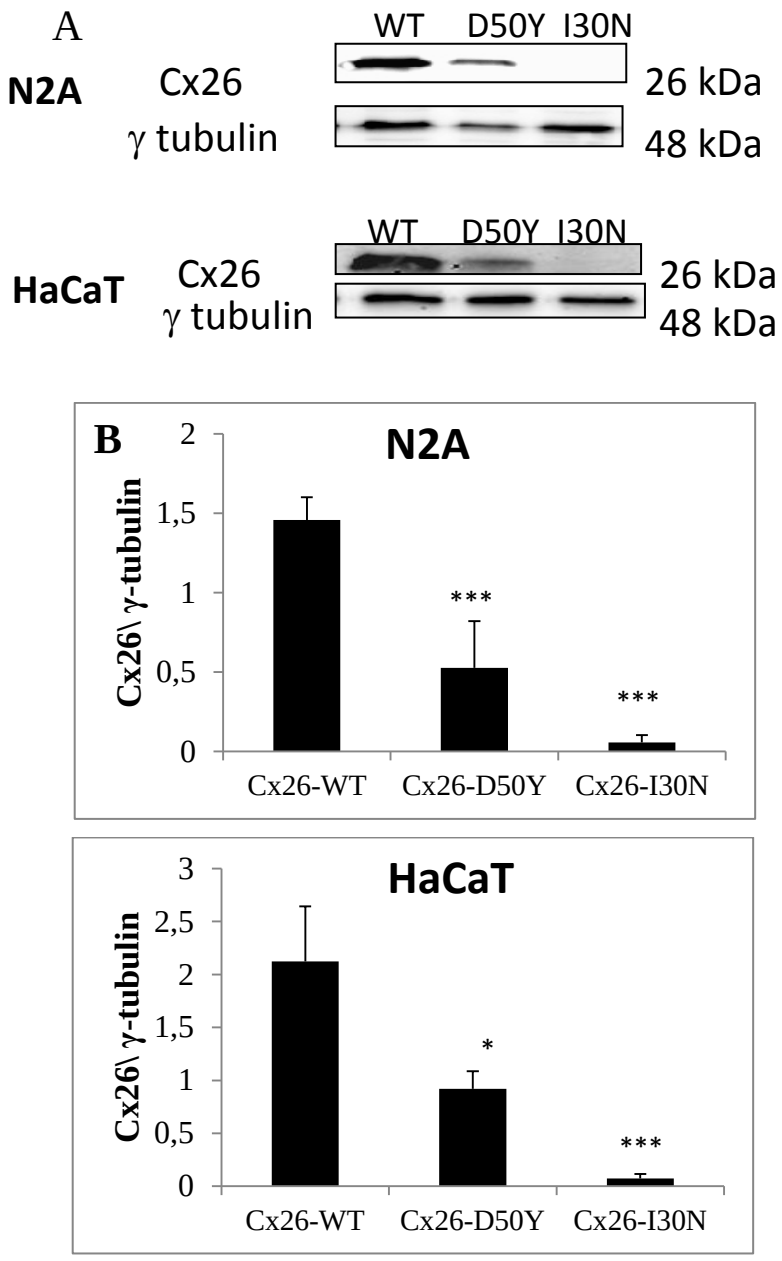

Figure 3.7. Western blot analysis of transfected N2A and HaCaT cells. A) Nitrocellulose membrane images of western blot results. Protein bands are Cx26 (26 kDa) and γ tubulin (48 kDa). γ tubulin was used as loading control. B) Graph indicates quantitative representation of protein bands on the membrane ($p<0.05$ *, $p< 0.01$ ***).

3.8. Effect of Cx26-I30N and D50Y Mutations on internal Ca^{2+} Content

After observation of localization and colocalization of Cx26-I30N and D50Y mutants in both HeLa and HaCaT cells, internal Ca^{2+} content measurements were performed to investigate permeability of aberrant hemichannels to Ca^{2+}. Ca^{2+} is a regulatory ion and maintain the epidermal homeostasis[92]. Ca^{2+} promotes keratinocyte differentiation and Cx26 mutations associated with KID syndrome cause Ca^{2+} deregulation[83]. Therefore, we aimed to examine effect of Cx26-I30N and D50Y on Ca^{2+} balance and measured internal Ca^{2+} content of Cx26 transfected cells.

Comparison of green signal intensity between Cx26-WT, I30N and D50Y conditions indicated that internal Ca^{2+} content increased in both Cx26-I30N and D50Y transfected cells. Results of N2A cells showed that cells with Cx26-I30N clone had 2.4 fold and cells with Cx26-D50Y clone had 2.3 fold increase in Ca2+ amount when compared with cells containing Cx26-WT (Figure 3.8 A). Elevation of Ca^{2+} content in Cx26-I30N and D50Y transfected cells were statistically significant ($p<0.01$). On the other hand, results of HaCaT cells indicated that cells with Cx26-I30N and D50Y clones had 1.4 fold increase in calcium amount with respect to Cx26-WT transfected cells (Figure 3.8 B). Elevation of Ca^{2+} content in Cx26-I30N and D50Y transfected cells were also statistically significant ($p<0.05$).

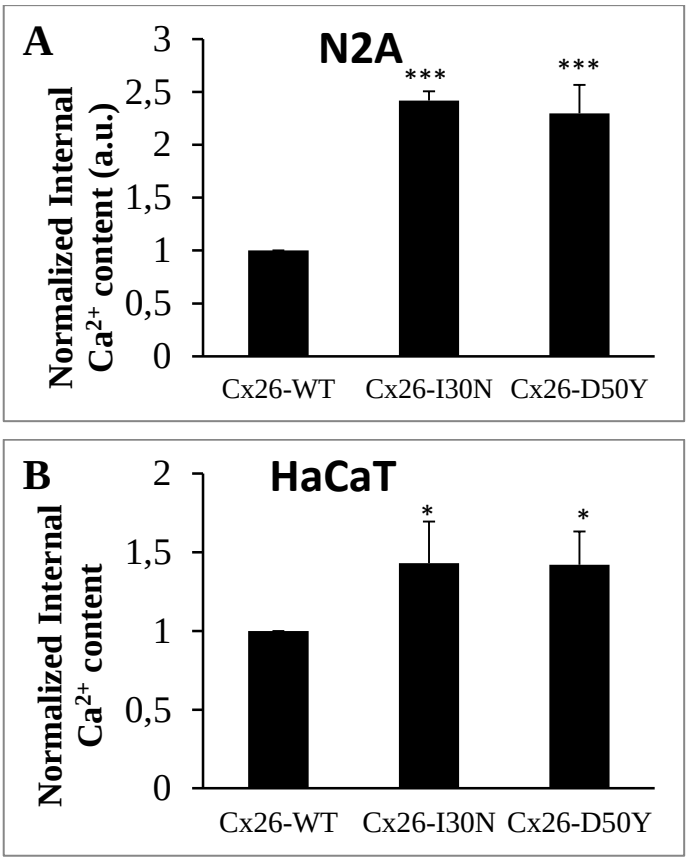

Figure 3.8. Internal Ca^{2+} measurement of transfected N2A and HaCaT cells. Fluo-3AM was used for measurement of internal Ca^{2+} content by flow cytometry. A) N2A cells were transfected with pCS2+Cx26-WT, I30N and D50Y constructs ($p<0.01$, ***). B) HaCaT cells were transfected with pCS2+Cx26-WT, I30N and D50Y constructs ($p<0.05$ *). Graphs shows normalized internal Ca^{2+} content of both transfected N2A and HaCaT cells.

3.9. Effect of Cx26-I30N and D50Y Mutations on ATP Release

After internal Ca^{2+} content measurement, ATP release assay was performed to observe effect of aberrant hemichannels formed by Cx26-I30N and D50Y mutations on ATP release. Changes in internal Ca^{2+} content can affect amount of released ATP from cells. Therefore, we aimed to observe ATP release property of aberrant hemichannels formed by Cx26-I30N and D50Y mutations. Result of ATP release assay showed that there was 3.8 and 4.7 fold decrease in amount of released ATP from N2A cells transfected with Cx26-I30N and D50Y clones when compared with cells transfected with Cx26-WT, respectively (Figure 3.9 A). ATP release was significantly decreased in N2A cells transfected with Cx26-I30N ($p<0.05$) and D50Y ($p<0.01$) constructs. On the other hand, result of ATP release assay indicated that there were 1.1 and 1.6 fold

increase in HaCaT cells transfected with Cx26-I30N and D50Y in comparison with cells having Cx26-WT clone (Figure 3.9 B). However, these differences between mutant and WT conditions were not statistically significant in HaCaT cells.

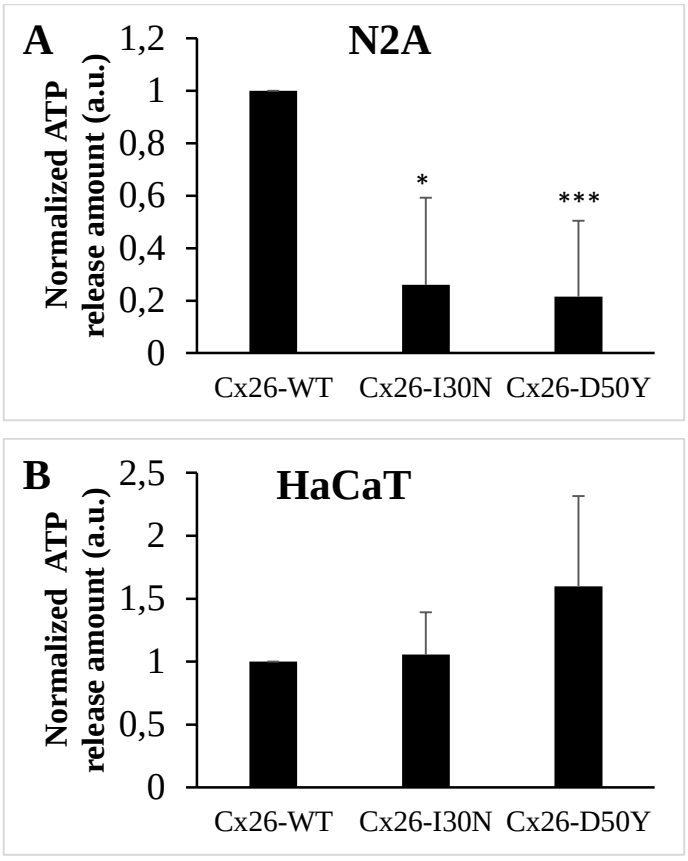

Figure 3.9. Measurement of released ATP from transfected N2A and HaCaT cells. ATP release assay was performed and released ATP amount was calculated. A) Graph shows released ATP amount from transfected N2A cells ($p<0.05$ *, $p<0.01$ ***). B) Graph shows released ATP amount from transfected HaCaT cells.

3.10. Effect of Cx26-I30N and D50Y Mutations on Cell Size

Cell size of N2A and HaCaT cells were measured by flow cytometry to observe size changes because of abnormal permeability of aberrant hemichannels. As a consequence of uptake of excess amount of Ca^{2+} inside the cell, cell size can increase. Therefore, we aimed to investigate effect of Cx26-I30N and D50Y mutations on cell size. Result of flow cytometry indicated that size of N2A cells transfected with Cx26-I30N and D50Y was elevated 1.12 fold and 1.04 fold, respectively when compared with

cells with Cx26-WT clone (Figure 3.10 A). N2A cells transfected with Cx26-I30N construct showed significant increase in cell size ($p<0.05$). On the other hand, size of HaCaT cells measured with flow cytometry indicated that there was no size change in HaCaT cells with Cx26-WT,Cx26-I30N and D50Y (Figure 3.10 B).

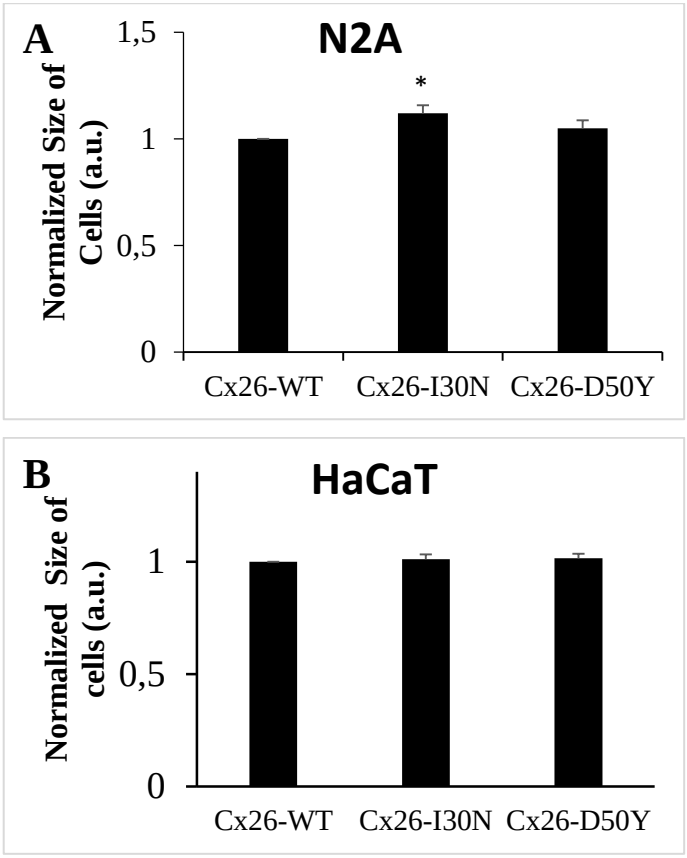

Figure 3.10: Cell size measurement of transfected N2A and HaCaT cells. Cell size was measured by flow cytometry. A) Graph indicates normalized size of N2A cells ($p<0.05$ *). B) Graph indicates normalized size of HaCaT cells.

3.11. Effect of Cx26-I30N and D50Y Mutations on Cell Death

After internal Ca^{2+} content measurement and ATP release assay, apoptosis assay was performed to observe the effect of aberrant hemichannels formed by Cx26-I30N and D50Y on cell death. Therefore, we determined apoptotic and necrotic cell numbers by flow cytometry to observe the effect of changed concentration of Ca^{2+} and released ATP amount inside the cells.

Apoptosis assay results showed there was 1.3 fold increase in number of late apoptotic cells transfected with Cx26-I30N construct (Figure 3.11 A). However, this

change was not statistically significant. On the other hand, number of necrotic cells transfected with Cx26-I30N and D50Y were 2.7 and 1.3 fold increase, respectively when compared with cells having Cx26-WT clone in N2A cells ($p < 0.05$) (Figure 3.11 B). In addition, apoptosis assay of HaCaT cells showed that there were 2.4 and 2.1 fold increase in the number of late apoptotic cells transfected with Cx26-I30N and D50Y clones, respectively when compared with cells having WT clone ($p < 0.05$) (Figure 3.11 C). Number of necrotic cells were increase 3.1 and 1,6 fold for Cx26-I30N and D50Y transfected HaCaT cells when compared with cells with WT ($p<0.05$) (Figure 3.11 D). Result of apoptosis assay showed that Cx26-I30N and D50Y mutations promoted late apoptotic and necrotic cell death.

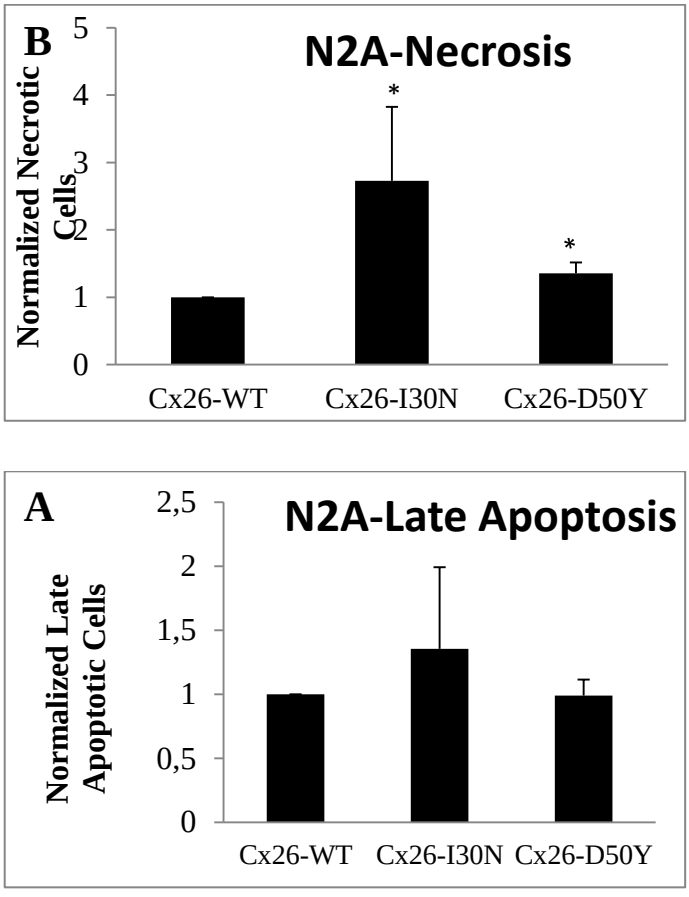

Figure 3.11. Apoptosis profile of transfected N2A and HaCaT cells. Apoptosis assay was performed with Annexin-V and 7-AAD apoptosis markers by flow cytometry. A) N2A cell number for late apoptotic stage. B) N2A cell number for necrotic stage. C) HaCaT cell number for late apoptotic stage. D) HaCaT cell number for necrotic stage ($p<0.05$ *, $p<0.01$ ***).

(Cont. on next page)

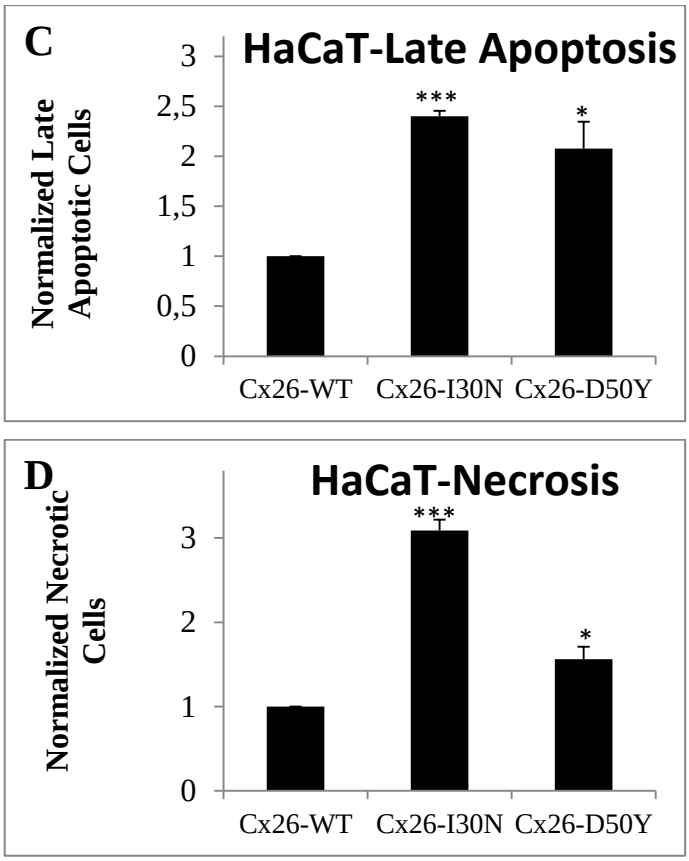

Figure 3.11 (cont.)

CHAPTER 4

DISCUSSION

In this study, we aimed to investigate functionality of aberrant hemichannels formed Cx26-I30N and D50Y mutations. Therefore, we performed immunostaining and co-immunostaining experiments to investigate cellular localization of Cx26-I30N and D50Y mutations. Results of immunostaining and coimmunostaining experiments indicated that there was Cx26-I30N and D50Y mutant protein expression and they were mainly localized in cytoplasm. Cx26-I30N and D50Y mutant proteins were unable to form gap junction channels at contact sites of adjacent cells and presence of other connexins did not affect their location. In addition, Cx26-I30N and D50Y mutant proteins accumulated in the Golgi apparatus in absence and presence of other connexins. After determination of localization of Cx26-I30N and D50Y mutant proteins, mRNA level expression of Cx26 and Cx43 with semi-quantitative RT-PCR and Cx26-I30N and D50Y protein synthesis level with western blot was investigated in N2A and HaCaT cells. Results showed that Cx26-I30N mRNA level decreased in HaCaT cells while Cx43 mRNA level increased. Cx26-I30N and D50Y mutations enhanced expression of Cx43. In addition, Cx26-I30N and D50Y protein levels were decreased in both N2A and HaCaT cells.

Cx26-I30N and D50Y mutant proteins form aberrant hemichannels. To investigate the permeability of aberrant hemichannels, we performed functional tests such as the measurement of internal Ca^{2+} content, ATP release assay and apoptosis assay. Results showed that aberrant hemichannels formed by Cx26-I30N and D50Y caused an increase in internal Ca^{2+} content and disrupted Ca^{2+} balance. In addition, released ATP amount decreased in N2A cells transfected with Cx26-I30N and D50Y. Furthermore, N2A cells having Cx26-I30N clone had larger cell size. Finally, apoptosis assay results showed that Cx26-I30N and D50Y mutations induced necrotic cell death.

Cx26-I30N and D50Y mutant proteins did not form gap junction plaques at the plasma membrane. There can be some reasons to prevent gap junction formation of Cx26-I30N and D50Y mutations. I30N and D50Y mutations are formed by single aminoacid substitutions. For I30N, isoleucine (I) at 30^{th} position is replaced with

asparagine (N) residue. Isoleucine is a nonpolar amino acid while asparagine is a polar amino acid. Also, their biochemical and molecular properties are different which can affect and then alter the interaction between amino acids and the protein folding. In addition, I30N mutation was found in the first transmembrane domain of Cx26 which has role in pore lining and oligomerization[20]. On the other hand, for D50Y mutation, aspartic acid at 50th position was replaced with tyrosine. Aspartic acid is a negatively charged polar amino acid whereas tyrosine is a nonpolar uncharged amino acid. Charge difference and size difference between amino acids can affect Cx26 folding. Moreover, aspartic acid at 50th location in Cx26 is highly conserved and it is found in first extracellular loop which has role in hemichannel docking[21]. Therefore, I30N and D50Y mutations can affect oligomerization and hemichannel docking function of Cx26 and therefore can prevent gap junction formation in N2A and HaCaT cells.

Trafficking of connexins is mediated by secretory pathway and accumulation of Cx26 mutants in the Golgi apparatus was also observed for other disease-associated mutations such as Cx26-D66H and R184Q in previous studies[47,48]. Golgi apparatus accumulation of Cx26 mutations can be caused by misfolding of Cx26 or trafficking defects[48]. However, exact mechanisms of accumulation in Golgi apparatus are not known. In our study, both Cx26-I30N and D50Y mutations were localized in the Golgi apparatus in both HeLa and HaCaT cells. This result indicated that Cx26-I30N and D50Y mutant proteins mostly localized in Golgi apparatus and presence of other connexins did not prevent Golgi apparatus accumulation of mutant proteins.

Cx26 mutations associated with KID syndrome can have trans-dominant effect on wild type Cx26 and other wild type connexins (Cx30 and Cx43)[82]. Homomeric hemichannels formed by Cx26 mutations are unable to form gap junction and, Cx26 mutations can affect the ability of Cx30 to form gap junction channels and therefore decrease GJIC[6,47]. On the other hand, some Cx26 mutations resulted in the formation of aberrant heteromeric hemichannels with wild type Cx43 and form gap junction[82].mRNA level of Cx26 and Cx43 indicated that mRNA expression of Cx26-I30N mutation decreased and expression of Cx43 increased significantly. This result showed that Cx26-I30N and D50Y mutations can increase the expression of Cx43.

In previous study, it was observed that both mRNA level and protein level of Cx26-P173R mutation was associated with non-syndromic hearing loss decreased[93]. Mutations in Cx26 can affect the half-life of the protein and the mRNA. In our results, mRNA level of Cx26-I30N clone and protein level of Cx26-I30N and D50Y decreased.

Decrease in the mRNA level of Cx26-I30N clone can be explained by the effect of the mutation on the stability of mRNA or its effect on the rapid degradation. In addition Cx26-D50Y protein level decreased because of decrease in mRNA level and Cx26-I30N protein level couldn't be determined because of antibody binding problem.

There is a Ca^{2+} gradient in the epidermis which is in the lowest level at basal layer and the highest at the corneum layer. This Ca^{2+} gradient is essential for proper differentiation of keratinocytes since Ca^{2+} gradient influences gene expression and protein function and protein interactions with each other. For example, low Ca^{2+} concentration induces keratin5 and keratin14 expression at the basal layer while higher Ca^{2+} concentration at the top induces involucrin expression which enhances differentiation of keratinocytes to form granuler layer. Disruption of this gradient diminishes keratinocyte differentiation and induces proliferation[92]. In previous study, Cx26-G11E and D50N mutations associated with KID syndrome showed increased Ca^{2+} content[83]. In our results, internal Ca^{2+} measurement of transfected N2A and HaCaT cells indicated that aberrant hemichannels formed by I30N and D50Y mutants also cause Ca^{2+} deregulation. Therefore, we can conclude that Ca^{2+} deregulation of Cx26-I30N and D50Y mutations may disrupt keratinocyte differentiation and cause development of KID syndrome.

In previous studies, it was indicated that aberrant hemichannels formed by KID syndrome associated Cx26 mutations changed amount of released ATP[94]. In our study, aberrant hemichannels formed by Cx26-I30N and D50Y mutations released less ATP than normal hemichannels formed by Cx26-WT in N2A cells. On the other hand, for HaCaT cells, amount of released ATP were not changed when cells transfected with Cx26-I30N and D50Y with comparison of Cx26-WT (Figure 3.9). In HaCaT cells, hemichannels formed by endogenous connexins may balance released ATP amount.

Previously, it was shown that Cx26-G45E mutation increased cell perimeter in keratinocytes and FACS analysis of Cx26-G11E transfected NHEK cells showed increased cell size when compared with cells transfected with Cx26-WT clone[79,83]. In addition, a short case report showed that patients with KID syndrome had swollen keratinocytes[95]. These results showed that KID syndrome related Cx26 mutations can affect the cell size. In our results, Cx26-I30N mutation also caused cell size increase in N2A cells but cell size increase in HaCaT cells transfected with Cx26-I30N and D50Y constructs were not observed. Keratinocytes are highly connected with each other

through a complex keratin cytoskeleton which can hold the cell shape in HaCaT cells [96] and this might account for the observed differences between N2A and HaCaT cells.

Many events in cell can induce apoptosis and necrosis such as abnormal transport of molecules across the plasma membrane. In addition, KID syndrome patients with necrosis were observed in previous studies[88,97]. Cx26-G45E mutation increased number of apoptotic cells in transfected cells[57]. Cx26-G11E mutation was observed to enhance necrosis[83]. Moreover, transgenic mice having Cx26-G45E mutation resulted in reduced viability[79]. In our results, Cx26-I30N and D50Y mutations were shown to cause an increase in late apoptosis and necrosis. Late apoptosis and necrosis can be induced by Ca^{2+} deregulation and changes in the amount of ATP in cells.

CHAPTER 5

CONCLUSION

In this study, we aimed to determine the functional effects of aberrant hemichannels formed by Cx26-I30N and D50Y mutations. We performed immunostaining and coimmunostaining experiments to examine localization of mutant proteins in cells. In addition, mRNA and protein levels of Cx26-I30N and D50Y clones were investigated. Lastly, functional analysis including internal Ca^{2+} content measurement, ATP release assay and apoptosis assay were performed.

Results indicated that Cx26-I30N and D50Y mutant proteins mainly localized in the Golgi apparatus. mRNA expression of *GJB2* gene with Cx26-I30N mutation was decreased and protein synthesis of Cx26-I30N and D50Y protein was decreased when compared with Cx26-WT mRNA and protein synthesis levels, respectively. In addition, Cx26-I30N and D50Y mutations disrupted Ca^{2+} balance and changed the amount of released ATP in N2A cells. Cell size of N2A with Cx26-I30N clone increased and Cx26-I30N and D50Y mutations increased necrotic cell death. With the light of these results, we can conclude that aberrant hemichannels formed by Cx26-I30N and D50Y mutations may induce apoptosis and necrosis because of deregulation of Ca^{2+} and/or ATP homeostasis in cells.

All in all, in this study, we determined functions of aberrant hemichannels formed by Cx26-I30N and D50Y mutations. Results showed that Cx26-I30N and D50Y formed aberrant hemichannels that can affect various cellular processes that can play role in the development of KID syndrome.

REFERENCES

1. Harris, A. L., Emerging issues of connexin channels: biophysics fills the gap. *Q Rev Biophys* **2001,** *34* (3), 325-472.

2. Phelan, P.; Starich, T. A., Innexins get into the gap. *Bioessays* **2001,** *23* (5), 388-96.

3. Lee, J. R.; White, T. W., Connexin-26 mutations in deafness and skin disease. *Expert Rev Mol Med* **2009,** *11*, e35.

4. Sohl, G.; Willecke, K., Gap junctions and the connexin protein family. *Cardiovasc Res* **2004,** *62* (2), 228-32.

5. Kleopa, K. A.; Sargiannidou, I., Connexins, gap junctions and peripheral neuropathy. *Neurosci Lett* **2015,** *596*, 27-32.

6. Mese, G.; Richard, G.; White, T. W., Gap junctions: basic structure and function. *J Invest Dermatol* **2007,** *127* (11), 2516-24.

7. Laird, D. W., The gap junction proteome and its relationship to disease. *Trends Cell Biol* **2010,** *20* (2), 92-101.

8. Saez, J. C.; Retamal, M. A.; Basilio, D.; Bukauskas, F. F.; Bennett, M. V., Connexin-based gap junction hemichannels: gating mechanisms. *Biochim Biophys Acta* **2005,** *1711* (2), 215-24.

9. Laird, D. W., Life cycle of connexins in health and disease. *Biochem J* **2006,** *394* (Pt 3), 527-43.

10. Mylvaganam, S.; Ramani, M.; Krawczyk, M.; Carlen, P. L., Roles of gap junctions, connexins, and pannexins in epilepsy. *Front Physiol* **2014,** *5*, 172.

11. Gerhart, S. V.; Jefferis, R.; Iovine, M. K., Cx40.8, a Cx43-like protein, forms gap junction channels inefficiently and may require Cx43 for its association at the plasma membrane. *FEBS Lett* **2009,** *583* (21), 3419-24.

12. Martin, P. E.; Easton, J. A.; Hodgins, M. B.; Wright, C. S., Connexins: sensors of epidermal integrity that are therapeutic targets. *FEBS Lett* **2014,** *588* (8), 1304-14.

13. Stewart, M. K.; Simek, J.; Laird, D. W., Insights into the role of connexins in mammary gland morphogenesis and function. *Reproduction* **2015,** *149* (6), R279-R290; 14. Goodenough, D. A.; Paul, D. L., Beyond the gap: functions of unpaired connexon channels. *Nat Rev Mol Cell Biol* **2003,** *4* (4), 285-94.

15. Hua, V. B.; Chang, A. B.; Tchieu, J. H.; Kumar, N. M.; Nielsen, P. A.; Saier, M. H., Jr., Sequence and phylogenetic analyses of 4 TMS junctional proteins of animals: connexins, innexins, claudins and occludins. *J Membr Biol* **2003,** *194* (1), 59-76.

16. Kumar, N. M.; Gilula, N. B., Molecular biology and genetics of gap junction channels. *Semin Cell Biol* **1992,** *3* (1), 3-16.

17. Sun, J.; Ahmad, S.; Chen, S.; Tang, W.; Zhang, Y.; Chen, P.; Lin, X., Cochlear gap junctions coassembled from Cx26 and 30 show faster intercellular Ca2+ signaling than homomeric counterparts. *Am J Physiol Cell Physiol* **2005,** *288* (3), C613-23.

18. Verheule, S.; Kaese, S., Connexin diversity in the heart: insights from transgenic mouse models. *Front Pharmacol* **2013,** *4*, 81.

19. Wonkam, A.; Noubiap, J. J.; Bosch, J.; Dandara, C.; Toure, G. B., Heterozygous p.Asp50Asn mutation in the GJB2 gene in two Cameroonian patients with keratitis-ichthyosis-deafness (KID) syndrome. *BMC Med Genet* **2013,** *14*, 81.

20. Maeda, S.; Nakagawa, S.; Suga, M.; Yamashita, E.; Oshima, A.; Fujiyoshi, Y.; Tsukihara, T., Structure of the connexin 26 gap junction channel at 3.5 A resolution. *Nature* **2009,** *458* (7238), 597-602.

21. Bao, X.; Chen, Y.; Reuss, L.; Altenberg, G. A., Functional expression in Xenopus oocytes of gap-junctional hemichannels formed by a cysteine-less connexin 43. *J Biol Chem* **2004,** *279* (11), 9689-92.

22. Hirst-Jensen, B. J.; Sahoo, P.; Kieken, F.; Delmar, M.; Sorgen, P. L., Characterization of the pH-dependent interaction between the gap junction protein connexin43 carboxyl terminus and cytoplasmic loop domains. *J Biol Chem* **2007,** *282* (8), 5801-13.

23. Bargiello, T. A.; Tang, Q.; Oh, S.; Kwon, T., Voltage-dependent conformational changes in connexin channels. *Biochim Biophys Acta* **2012,** *1818* (8), 1807-22.

24. Abascal, F.; Zardoya, R., Evolutionary analyses of gap junction protein families. *Biochim Biophys Acta* **2013,** *1828* (1), 4-14.

25. Beardslee, M. A.; Laing, J. G.; Beyer, E. C.; Saffitz, J. E., Rapid turnover of connexin43 in the adult rat heart. *Circ Res* **1998,** *83* (6), 629-35.

26. Thomas, T.; Jordan, K.; Simek, J.; Shao, Q.; Jedeszko, C.; Walton, P.; Laird, D. W., Mechanisms of Cx43 and Cx26 transport to the plasma membrane and gap junction regeneration. *J Cell Sci* **2005,** *118* (Pt 19), 4451-62.

27. Musil, L. S.; Le, A. C.; VanSlyke, J. K.; Roberts, L. M., Regulation of connexin degradation as a mechanism to increase gap junction assembly and function. *J Biol Chem* **2000,** *275* (33), 25207-15.

28. Smith, T. D.; Mohankumar, A.; Minogue, P. J.; Beyer, E. C.; Berthoud, V. M.; Koval, M., Cytoplasmic amino acids within the membrane interface region influence connexin oligomerization. *J Membr Biol* **2012,** *245* (5-6), 221-30.

29. Das Sarma, J.; Das, S.; Koval, M., Regulation of connexin43 oligomerization is saturable. *Cell Commun Adhes* **2005,** *12* (5-6), 237-47.

30. Shaw, R. M.; Fay, A. J.; Puthenveedu, M. A.; von Zastrow, M.; Jan, Y. N.; Jan, L. Y., Microtubule plus-end-tracking proteins target gap junctions directly from the cell interior to adherens junctions. *Cell* **2007,** *128* (3), 547-60.

31. Thevenin, A. F.; Kowal, T. J.; Fong, J. T.; Kells, R. M.; Fisher, C. G.; Falk, M. M., Proteins and mechanisms regulating gap-junction assembly, internalization, and degradation. *Physiology (Bethesda)* **2013,** *28* (2), 93-116.

32. Falk, M. M.; Baker, S. M.; Gumpert, A. M.; Segretain, D.; Buckheit, R. W., 3rd, Gap junction turnover is achieved by the internalization of small endocytic double-membrane vesicles. *Mol Biol Cell* **2009,** *20* (14), 3342-52.

33. Falk, M. M.; Fong, J. T.; Kells, R. M.; O'Laughlin, M. C.; Kowal, T. J.; Thevenin, A. F., Degradation of endocytosed gap junctions by autophagosomal and endo-/lysosomal pathways: a perspective. *J Membr Biol* **2012,** *245* (8), 465-76.

34. Piehl, M.; Lehmann, C.; Gumpert, A.; Denizot, J. P.; Segretain, D.; Falk, M. M., Internalization of large double-membrane intercellular vesicles by a clathrin-dependent endocytic process. *Mol Biol Cell* **2007,** *18* (2), 337-47.

35. Kjenseth, A.; Fykerud, T.; Rivedal, E.; Leithe, E., Regulation of gap junction intercellular communication by the ubiquitin system. *Cell Signal* **2010,** *22* (9), 1267-73.

36. Bejarano, E.; Girao, H.; Yuste, A.; Patel, B.; Marques, C.; Spray, D. C.; Pereira, P.; Cuervo, A. M., Autophagy modulates dynamics of connexins at the plasma membrane in a ubiquitin-dependent manner. *Mol Biol Cell* **2012,** *23* (11), 2156-69.

37. Gerido, D. A.; White, T. W., Connexin disorders of the ear, skin, and lens. *Biochim Biophys Acta* **2004,** *1662* (1-2), 159-70.

38. Kim, M. S.; Gloor, G. B.; Bai, D., The distribution and functional properties of Pelizaeus-Merzbacher-like disease-linked Cx47 mutations on Cx47/Cx47 homotypic and Cx47/Cx43 heterotypic gap junctions. *Biochem J* **2013,** *452* (2), 249-58.

39. Liu, X. Z.; Xia, X. J.; Xu, L. R.; Pandya, A.; Liang, C. Y.; Blanton, S. H.; Brown, S. D.; Steel, K. P.; Nance, W. E., Mutations in connexin31 underlie recessive as well as dominant non-syndromic hearing loss. *Hum Mol Genet* **2000,** *9* (1), 63-7.

40. Wilcox, S. A.; Saunders, K.; Osborn, A. H.; Arnold, A.; Wunderlich, J.; Kelly, T.; Collins, V.; Wilcox, L. J.; McKinlay Gardner, R. J.; Kamarinos, M.; Cone-Wesson, B.; Williamson, R.; Dahl, H. H., High frequency hearing loss correlated with mutations in the GJB2 gene. *Hum Genet* **2000,** *106* (4), 399-405.

41. Wilgoss, A.; Leigh, I. M.; Barnes, M. R.; Dopping-Hepenstal, P.; Eady, R. A.; Walter, J. M.; Kennedy, C. T.; Kelsell, D. P., Identification of a novel mutation R42P in the gap junction protein beta-3 associated with autosomal dominant erythrokeratoderma variabilis. *J Invest Dermatol* **1999,** *113* (6), 1119-22.

42. Jani-Acsadi, A.; Ounpuu, S.; Pierz, K.; Acsadi, G., Pediatric Charcot-Marie-Tooth Disease. *Pediatr Clin North Am* **2015,** *62* (3), 767-786.

43. Beyer, E. C.; Berthoud, V. M., Connexin hemichannels in the lens. *Front Physiol* **2014,** *5*, 20.

44. Kelly, J. J.; Simek, J.; Laird, D. W., Mechanisms linking connexin mutations to human diseases. *Cell Tissue Res* **2015,** *360* (3), 701-21.

45. Kudo, T.; Ikeda, K.; Kure, S.; Matsubara, Y.; Oshima, T.; Watanabe, K.; Kawase, T.; Narisawa, K.; Takasaka, T., Novel mutations in the connexin 26 gene (GJB2) responsible for childhood deafness in the Japanese population. *Am J Med Genet* **2000,** *90* (2), 141-5.

46. Zelante, L.; Gasparini, P.; Estivill, X.; Melchionda, S.; D'Agruma, L.; Govea, N.; Mila, M.; Monica, M. D.; Lutfi, J.; Shohat, M.; Mansfield, E.; Delgrosso, K.; Rappaport, E.; Surrey, S.; Fortina, P., Connexin26 mutations associated with the most common form of non-syndromic neurosensory autosomal recessive deafness (DFNB1) in Mediterraneans. *Hum Mol Genet* **1997,** *6* (9), 1605-9.

47. Su, C. C.; Li, S. Y.; Su, M. C.; Chen, W. C.; Yang, J. J., Mutation R184Q of connexin 26 in hearing loss patients has a dominant-negative effect on connexin 26 and connexin 30. *Eur J Hum Genet* **2010,** *18* (9), 1061-4.

48. Thomas, T.; Telford, D.; Laird, D. W., Functional domain mapping and selective trans-dominant effects exhibited by Cx26 disease-causing mutations. *J Biol Chem* **2004,** *279* (18), 19157-68.

49. Gong, X. Q.; Nakagawa, S.; Tsukihara, T.; Bai, D., A mechanism of gap junction docking revealed by functional rescue of a human-disease-linked connexin mutant. *J Cell Sci* **2013,** *126* (Pt 14), 3113-20.

50. Mani, R. S.; Ganapathy, A.; Jalvi, R.; Srikumari Srisailapathy, C. R.; Malhotra, V.; Chadha, S.; Agarwal, A.; Ramesh, A.; Rangasayee, R. R.; Anand, A., Functional consequences of novel connexin 26 mutations associated with hereditary hearing loss. *Eur J Hum Genet* **2009,** *17* (4), 502-9.

51. Yoshikawa, S.; Kawano, A.; Hayashi, C.; Nishiyama, N.; Kawaguchi, S.; Furuse, H.; Ikeda, K.; Suzuki, M.; Nakagawa, M., The clinical features of patients with the homozygous 235delC and the compound-heterozygous Y136X/G45E of the GJB2 mutations (Connexin 26) in cochlear implant recipients. *Auris Nasus Larynx* **2011,** *38* (4), 444-9.

52. Beltramello, M.; Piazza, V.; Bukauskas, F. F.; Pozzan, T.; Mammano, F., Impaired permeability to Ins(1,4,5)P3 in a mutant connexin underlies recessive hereditary deafness. *Nat Cell Biol* **2005,** *7* (1), 63-9.

53. Beyer, E. C.; Ebihara, L.; Berthoud, V. M., Connexin mutants and cataracts. *Front Pharmacol* **2013,** *4*, 43.

54. Churko, J. M.; Langlois, S.; Pan, X.; Shao, Q.; Laird, D. W., The potency of the fs260 connexin43 mutant to impair keratinocyte differentiation is distinct from other disease-linked connexin43 mutants. *Biochem J* **2010,** *429* (3), 473-83.

55. Diestel, S.; Richard, G.; Doring, B.; Traub, O., Expression of a connexin31 mutation causing erythrokeratodermia variabilis is lethal for HeLa cells. *Biochem Biophys Res Commun* **2002,** *296* (3), 721-8.

56. Sanchez, H. A.; Mese, G.; Srinivas, M.; White, T. W.; Verselis, V. K., Differentially altered Ca2+ regulation and Ca2+ permeability in Cx26 hemichannels formed by the A40V and G45E mutations that cause keratitis ichthyosis deafness syndrome. *J Gen Physiol* **2010,** *136* (1), 47-62.

57. Stong, B. C.; Chang, Q.; Ahmad, S.; Lin, X., A novel mechanism for connexin 26 mutation linked deafness: cell death caused by leaky gap junction hemichannels. *Laryngoscope* **2006,** *116* (12), 2205-10.

58. Rouan, F.; White, T. W.; Brown, N.; Taylor, A. M.; Lucke, T. W.; Paul, D. L.; Munro, C. S.; Uitto, J.; Hodgins, M. B.; Richard, G., trans-dominant inhibition of connexin-43 by mutant connexin-26: implications for dominant connexin disorders affecting epidermal differentiation. *J Cell Sci* **2001,** *114* (Pt 11), 2105-13.

59. Gemel, J.; Valiunas, V.; Brink, P. R.; Beyer, E. C., Connexin43 and connexin26 form gap junctions, but not heteromeric channels in co-expressing cells. *J Cell Sci* **2004,** *117* (Pt 12), 2469-80.

60. Dobrowolski, R.; Sommershof, A.; Willecke, K., Some oculodentodigital dysplasia-associated Cx43 mutations cause increased hemichannel activity in addition to deficient gap junction channels. *J Membr Biol* **2007,** *219* (1-3), 9-17.

61. Ren, Q.; Riquelme, M. A.; Xu, J.; Yan, X.; Nicholson, B. J.; Gu, S.; Jiang, J. X., Cataract-causing mutation of human connexin 46 impairs gap junction, but increases hemichannel function and cell death. *PLoS One* **2013,** *8* (9), e74732.

62. Gerido, D. A.; DeRosa, A. M.; Richard, G.; White, T. W., Aberrant hemichannel properties of Cx26 mutations causing skin disease and deafness. *Am J Physiol Cell Physiol* **2007,** *293* (1), C337-45.

63. Dai, P.; Yu, F.; Han, B.; Liu, X.; Wang, G.; Li, Q.; Yuan, Y.; Liu, X.; Huang, D.; Kang, D.; Zhang, X.; Yuan, H.; Yao, K.; Hao, J.; He, J.; He, Y.; Wang, Y.; Ye, Q.; Yu, Y.; Lin, H.; Liu, L.; Deng, W.; Zhu, X.; You, Y.; Cui, J.; Hou, N.; Xu, X.; Zhang, J.; Tang, L.; Song, R.; Lin, Y.; Sun, S.; Zhang, R.; Wu, H.; Ma, Y.; Zhu, S.; Wu, B. L.; Han, D.; Wong, L. J., GJB2 mutation spectrum in 2,063 Chinese patients with nonsyndromic hearing impairment. *J Transl Med* **2009,** *7*, 26.

64. Petit, C.; Levilliers, J.; Hardelin, J. P., Molecular genetics of hearing loss. *Annu Rev Genet* **2001,** *35*, 589-646.

65. Yan, D.; Liu, X. Z., Cochlear molecules and hereditary deafness. *Front Biosci* **2008,** *13*, 4972-83.

66. Antoniadi, T.; Gronskov, K.; Sand, A.; Pampanos, A.; Brondum-Nielsen, K.; Petersen, M. B., Mutation analysis of the GJB2 (connexin 26) gene by DGGE in Greek patients with sensorineural deafness. *Hum Mutat* **2000,** *16* (1), 7-12.

67. Richard, G., Connexin disorders of the skin. *Clin Dermatol* **2005,** *23* (1), 23-32.

68. Al Fahaad, H., Keratitis-ichthyosis-deafness syndrome: first affected family reported in the Middle East. *Int Med Case Rep J* **2014,** *7*, 63-6.

69. Janecke, A. R.; Hennies, H. C.; Gunther, B.; Gansl, G.; Smolle, J.; Messmer, E. M.; Utermann, G.; Rittinger, O., GJB2 mutations in keratitis-ichthyosis-deafness syndrome including its fatal form. *Am J Med Genet A* **2005,** *133A* (2), 128-31.

70. Grob, J. J.; Breton, A.; Bonafe, J. L.; Sauvan-Ferdani, M.; Bonerandi, J. J., Keratitis, ichthyosis, and deafness (KID) syndrome. Vertical transmission and death from multiple squamous cell carcinomas. *Arch Dermatol* **1987,** *123* (6), 777-82.

71. Olah, A.; Szollosi, A. G.; Biro, T., The channel physiology of the skin. *Rev Physiol Biochem Pharmacol* **2012,** *163*, 65-131.

72. Eckert, R. L.; Rorke, E. A., Molecular biology of keratinocyte differentiation. *Environ Health Perspect* **1989,** *80*, 109-16.

73. Tu, C. L.; Bikle, D. D., Role of the calcium-sensing receptor in calcium regulation of epidermal differentiation and function. *Best Pract Res Clin Endocrinol Metab* **2013,** *27* (3), 415-27.

74. Brissette, J. L.; Kumar, N. M.; Gilula, N. B.; Hall, J. E.; Dotto, G. P., Switch in gap junction protein expression is associated with selective changes in junctional permeability during keratinocyte differentiation. *Proc Natl Acad Sci U S A* **1994,** *91* (14), 6453-7.

75. Lucke, T.; Choudhry, R.; Thom, R.; Selmer, I. S.; Burden, A. D.; Hodgins, M. B., Upregulation of connexin 26 is a feature of keratinocyte differentiation in hyperproliferative epidermis, vaginal epithelium, and buccal epithelium. *J Invest Dermatol* **1999,** *112* (3), 354-61.

76. Kandyba, E. E.; Hodgins, M. B.; Martin, P. E., A murine living skin equivalent amenable to live-cell imaging: analysis of the roles of connexins in the epidermis. *J Invest Dermatol* **2008,** *128* (4), 1039-49.

77. Sanchez, H. A.; Villone, K.; Srinivas, M.; Verselis, V. K., The D50N mutation and syndromic deafness: altered Cx26 hemichannel properties caused by effects on the pore and intersubunit interactions. *J Gen Physiol* **2013,** *142* (1), 3-22.

78. Koppelhus, U.; Tranebjaerg, L.; Esberg, G.; Ramsing, M.; Lodahl, M.; Rendtorff, N. D.; Olesen, H. V.; Sommerlund, M., A novel mutation in the connexin 26 gene (GJB2) in a child with clinical and histological features of keratitis-ichthyosis-deafness (KID) syndrome. *Clin Exp Dermatol* **2011,** *36* (2), 142-8.

79. Mese, G.; Sellitto, C.; Li, L.; Wang, H. Z.; Valiunas, V.; Richard, G.; Brink, P. R.; White, T. W., The Cx26-G45E mutation displays increased hemichannel activity in a mouse model of the lethal form of keratitis-ichthyosis-deafness syndrome. *Mol Biol Cell* **2011,** *22* (24), 4776-86.

80. Mhaske, P. V.; Levit, N. A.; Li, L.; Wang, H. Z.; Lee, J. R.; Shuja, Z.; Brink, P. R.; White, T. W., The human Cx26-D50A and Cx26-A88V mutations causing keratitis-ichthyosis-deafness syndrome display increased hemichannel activity. *Am J Physiol Cell Physiol* **2013,** *304* (12), C1150-8.

81. Lee, J. R.; Derosa, A. M.; White, T. W., Connexin mutations causing skin disease and deafness increase hemichannel activity and cell death when expressed in Xenopus oocytes. *J Invest Dermatol* **2009,** *129* (4), 870-8.

82. Garcia, I. E.; Maripillan, J.; Jara, O.; Ceriani, R.; Palacios-Munoz, A.; Ramachandran, J.; Olivero, P.; Perez-Acle, T.; Gonzalez, C.; Saez, J. C.; Contreras, J. E.; Martinez, A. D., Keratitis-ichthyosis-deafness syndrome-associated cx26 mutants produce nonfunctional gap junctions but hyperactive hemichannels when co-expressed with wild type cx43. *J Invest Dermatol* **2015,** *135* (5), 1338-47.

83. Terrinoni, A.; Codispoti, A.; Serra, V.; Didona, B.; Bruno, E.; Nistico, R.; Giustizieri, M.; Alessandrini, M.; Campione, E.; Melino, G., Connexin 26 (GJB2) mutations, causing KID Syndrome, are associated with cell death due to calcium gating deregulation. *Biochem Biophys Res Commun* **2010,** *394* (4), 909-14.

84. Schutz, M.; Auth, T.; Gehrt, A.; Bosen, F.; Korber, I.; Strenzke, N.; Moser, T.; Willecke, K., The connexin26 S17F mouse mutant represents a model for the human hereditary keratitis-ichthyosis-deafness syndrome. *Hum Mol Genet* **2011,** *20* (1), 28-39.

85. Bay, V., Characterization of connexin 26 mutations causing hereditary skin disorders. **2013**.

86. Bolte, S.; Cordelieres, F. P., A guided tour into subcellular colocalization analysis in light microscopy. *J Microsc-Oxford* **2006,** *224*, 213-232.

87. Cao, F.; Eckert, R.; Elfgang, C.; Nitsche, J. M.; Snyder, S. A.; DF, H. u.; Willecke, K.; Nicholson, B. J., A quantitative analysis of connexin-specific permeability differences of gap junctions expressed in HeLa transfectants and Xenopus oocytes. *J Cell Sci* **1998,** *111 (Pt 1)*, 31-43.

88. Arndt, S.; Aschendorff, A.; Schild, C.; Beck, R.; Maier, W.; Laszig, R.; Birkenhager, R., A novel dominant and a de novo mutation in the GJB2 gene (connexin-26) cause keratitis-ichthyosis-deafness syndrome: implication for cochlear implantation. *Otol Neurotol* **2010,** *31* (2), 210-5.

89. Fitzgerald, D. J.; Fusenig, N. E.; Boukamp, P.; Piccoli, C.; Mesnil, M.; Yamasaki, H., Expression and function of connexin in normal and transformed human keratinocytes in culture. *Carcinogenesis* **1994,** *15* (9), 1859-65.

90. Wenzel, K.; Manthey, D.; Willecke, K.; Grzeschik, K. H.; Traub, O., Human gap junction protein connexin31: molecular cloning and expression analysis. *Biochem Biophys Res Commun* **1998,** *248* (3), 910-5.

91. Segretain, D.; Falk, M. M., Regulation of connexin biosynthesis, assembly, gap junction formation, and removal. *Biochim Biophys Acta* **2004,** *1662* (1-2), 3-21.

92. Bikle, D. D.; Oda, Y.; Xie, Z., Calcium and 1,25(OH)2D: interacting drivers of epidermal differentiation. *J Steroid Biochem Mol Biol* **2004,** *89-90* (1-5), 355-60.

93. Thonnissen, E.; Rabionet, R.; Arbones, M. L.; Estivill, X.; Willecke, K.; Ott, T., Human connexin26 (GJB2) deafness mutations affect the function of gap junction channels at different levels of protein expression. *Hum Genet* **2002,** *111* (2), 190-7.

94. Levit, N. A.; Mese, G.; Basaly, M. G.; White, T. W., Pathological hemichannels associated with human Cx26 mutations causing Keratitis-Ichthyosis-Deafness syndrome. *Biochim Biophys Acta* **2012,** *1818* (8), 2014-9.

95. Sbidian, E.; Feldmann, D.; Bengoa, J.; Fraitag, S.; Abadie, V.; de Prost, Y.; Bodemer, C.; Hadj-Rabia, S., Germline mosaicism in keratitis-ichthyosis-deafness syndrome: pre-natal diagnosis in a familial lethal form. *Clin Genet* **2010,** *77* (6), 587-92.

96. Breitkreutz, D.; Boukamp, P.; Ryle, C. M.; Stark, H. J.; Roop, D. R.; Fusenig, N. E., Epidermal morphogenesis and keratin expression in c-Ha-ras-transfected tumorigenic clones of the human HaCaT cell line. *Cancer Res* **1991,** *51* (16), 4402-9.

97. Coggshall, K.; Farsani, T.; Ruben, B.; McCalmont, T. H.; Berger, T. G.; Fox, L. P.; Shinkai, K., Keratitis, ichthyosis, and deafness syndrome: a review of infectious and neoplastic complications. *J Am Acad Dermatol* **2013,** *69* (1), 127-34.